In situ oxygen-isotope, major-, and trace-element constraints on the metasomatic modification and crustal origin of a diamondiferous eclogite from Roberts Victor, Kaapvaal Craton

Riches[1*,†], A. J. V., Ickert[1,2], R. B., Pearson[1], D. G., Stern[1], R. A., Jackson[3], S. E., Ishikawa[4], A., Kjarsgaard[3], B. A., and Gurney[5], J.J.

[1]Department of Earth and Atmospheric Sciences, University of Alberta, Edmonton, AB, T6G 2E3, Canada.

[2]Scottish Universities Environmental Research Centre, Scottish Enterprise Technology Research Park, Rankine Avenue, East Kilbride, G75 0QF.

[3]Geological Survey of Canada, Ottawa, Canada

[4]Department of Earth Science and Astronomy, The University of Tokyo at Komaba, Tokyo, 153-8902, Japan.

[5]Department of Geological Sciences, University of Cape Town, Rondebosch, 7700, Republic of South Africa.

[†]Currently at: Department of Earth Sciences, University of Durham, Durham, DH1 3LE, United Kingdom.

*corresponding author: amy.j.riches@durham.ac.uk

phone: +44 191 33 42346

Accepted: Geochimica et Cosmochimica Acta

Draft: 16th November 2015

Keywords: Eclogite, Achaean Crust/Mantle, Subduction, Oxygen Isotopes, Diamond.

Word Count: 5,887 main text + 430 abstract

Figure Count: 8

Table Count: 0 (supplementary files)

Reference Total: 117

Appended Materials: Data table (Appendices A + B, excel), and supplementary text + figures (Appendix C)

Abstract (430 words)

A subducted oceanic crustal origin for most eclogite xenoliths in kimberlites has long been a cornerstone of tectonic models for craton development. However, eclogite xenoliths often have protracted and complex histories involving multiple metasomatic events that could overprint some of the key geochemical indicators typically taken as evidence of a subducted origin (e,g, garnet δ^{18}O-values and mineral $^{87}Sr/^{86}Sr$ compositions). To assess the potential for disturbance of oxygen isotopic compositions in mantle eclogites via diamond-forming and other possible metasomatic fluids, we have conducted a multi-technique *in situ* study of a diamondiferous eclogite xenolith from the Roberts Victor kimberlite, S. Africa. Using SIMS we provide the first texturally-controlled *in situ* measurements of δ^{18}O-values in eclogitic garnet in close proximity to diamond.

Garnet and clinopyroxene modal proportions are heterogeneous in the xenolith and garnet compositions vary from Mg# = 75.8-79.2; grossular proportions = 8.05-10.14 mol. %, and omphacitic pyroxene has Jd_{13-24} and Mg# = 86.6-90.0. Rare earth element patterns of minerals across the xenolith, including grains close to diamond, are typical LREE-depleted garnets and markedly LREE-enriched pyroxenes. These silicate minerals also record detectable intra- and inter-grain LREE abundance variations. Clinopyroxenes of the studied xenoliths show HFSE and Sr abundance variations that are decoupled from LREE contents and major-element variations.

Mineralogical constraints and bulk-rock reconstructions indicate that the studied sample likely experienced selective incompatible element enrichment during small-volume (<<0.03 wt. %) infiltration of metasomatic fluid(s) potentially linked to ancient diamond evolution. Intra-

grain major-element, LREE and HFSE variations in clinopyroxene resulted from late-stage metasomatism. Oxygen isotope compositions in garnet are decoupled from all major- and trace-element variations, with garnet $\delta^{18}O$-values being uniform across the xenolith in a wide variety of textural settings. Garnet $\delta^{18}O$-values of 6.5 ± 0.2 ‰ are higher than the mean (5.19 ± 0.26 ‰) of the mantle garnet range (4.8-5.5 ‰).

Modelling of the buffering effect of mantle peridotite on CO_2-rich and H_2O-rich metasomatic fluids at temperatures within the diamond stability field indicates that the likelihood of a metasomatic fluid with exotic oxygen isotopic composition arriving at a mantle eclogite body with its isotopic composition unmodified, after percolative flow through dominantly peridotitic mantle at great depth, is very low. As we find no evidence of metasomatically induced garnet oxygen isotope variations in the studied diamondiferous eclogite xenolith we conclude that the most likely origin for the elevated garnet $\delta^{18}O$-values is via inheritance from a crustal protolith altered at relatively low temperatures. These results have broader relevance and support the hypothesis of a low-pressure protolith for mantle eclogite xenoliths, demonstrating the robust nature of garnet oxygen isotope compositions – even in diamond-bearing eclogites.

Keywords: Eclogite, Achaean Crust/Mantle, Subduction, Oxygen Isotopes, Diamond.

Main Text (5,727)

1. Introduction

The origins of kimberlite-borne eclogite xenoliths that are erupted through cratons have been debated for the last 30 years or more (e.g., MacGregor and Manton, 1986; Hatton and Gurney, 1987; Jacob *et al.*, 1994; Beard *et al.*, 1996; Jacob and Foley, 1999; Schmidberger *et al.*, 2007; Viljoen *et al.*, 2005; Aulbach *et al.*, 2007; Gurney *et al.*, 2010; Huang *et al.*, 2012; Shu *et al.*, 2014). Eclogites are volumetrically dominated by garnet and omphacitic pyroxene, and are generally considered as meta-igneous rocks having broadly basaltic bulk-rock compositions. Eclogites sampled as xenoliths preserve mineralogical and cryptic geochemical records of complex and protracted lithospheric mantle histories (e.g., Heaman *et al.*, 2002, 2006). Broad analogies have been drawn between mantle eclogite xenoliths sampled from depth and crustal eclogites that generally occur in orogenic settings, but which have distinct metamorphic histories (e.g., Coleman *et al.*, 1965; Nadaeu *et al.*, 1993; Baker *et al.*, 1997; Zack *et al.*, 2002; Zheng *et al.*, 2003; Konrad-Schmolke *et al.*, 2008). Critically, the distribution of oxygen isotope compositions of eclogite xenolith garnets, with $\delta^{18}O$-values ranging significantly above and below canonical mantle values, have drawn analogies with bulk-rock compositions reported for shallow-level ophiolite and mid-ocean ridge basalt (MORB) sequences altered by fluids at relatively low-temperatures. As such, these variations are often cited as evidence supporting a recycled crustal origin (e.g., Jagoutz *et al.*, 1984; Neal and Taylor, 1990; Neal *et al.*, 1990; Snyder *et al.*, 1995, 1997; Schulze *et al.*, 2000; Barth *et al.*, 2001; Jacob *et al.*, 2003; Spetsius *et al.*, 2008; Riches *et al.*, 2010; Tappe *et al.*, 2011; Carmody *et al.*, 2013; Pernet-Fisher *et al.*, 2014). Prior studies of oxygen isotope compositions of eclogite garnets have, however, largely employed multi-grain conventional-fluorination methods and laser-fluorination approaches on

mg-sized garnet fragments, which will result in compositional averages of larger garnet volumes. In addition, garnet-clinopyroxene modal banding and wide-spread evidence for cryptic metasomatism linked to the passage of incompatible-element-rich fluids ± diamond occurrences in eclogite xenoliths (e.g., Taylor *et al.*, 1996, 2000; Ishikawa *et al.*, 2008a-b; Spetsius and Taylor, 2008; Liu *et al*., 2009; Smart *et al*., 2009) lead some scientists to question the primary nature of garnet δ^{18}O-compositions (e.g., Huang *et al.*, 2014). The potential for eclogite garnet oxygen isotope compositions being of metasomatic origin has profound implications for the hypothesis of a subducted crustal origin for eclogite xenolith protoliths (e.g., Helmstaedt and Doig; 1975; Jacob, 2004) and warrants further study.

To assess intra-sample garnet oxygen isotope homogeneity and thereby test the validity of conclusions drawn from conventional- and laser-fluorination studies, which are considered fundamental evidence supporting the subduction origin of mantle eclogites, we selected a diamondiferous eclogite xenolith from the Roberts Victor kimberlite (**Fig. 1**) and utilised new generation secondary-ion mass spectrometry (SIMS) to obtain highly precise *in situ* garnet oxygen isotope data for texturally constrained grains at small spatial scales and low total volumes (15 μm spot diameter of 1-2 μm depth; << 5 ng; e.g., Page *et al.*, 2010; Ickert and Stern, 2013). This sample exhibited significant variation in diamond content, silicate mineral texture and mineral chemistry, enabling inter- and intra-grain garnet oxygen isotope variation to be assessed in the context of macro- and grain-scale textural and mineral chemical variations. Significantly, our study includes the first report of *in situ* δ^{18}O-compositions of garnet grains adjacent to diamond in eclogite, allowing us to investigate the potential effects of diamond-forming fluids on garnet oxygen isotope compositions. These data are supplemented by *in situ*

84 major- and trace-element abundance data of garnets and coexisting phases in garnet-rich and
85 clinopyroxene-rich portions of eclogite 09RV09 from the Roberts Victor kimberlite pipe.

86 **2. Analytical Methods**

87 **2.1 Sample preparation**

88 The studied eclogite xenolith, 09RV09 (total mass ~160 g), is from the Roberts Victor mine,
89 South Africa. The sample was selected on the basis of; 1) its relatively fresh appearance; 2) the
90 presence of diamonds, and; 3) heterogeneously distributed zones with varying modal proportions
91 of garnet and clinopyroxene. A 37 g slice derived from this diamondiferous-eclogite (**Fig. 2**)
92 was used for our study. This carefully examined slice contains zones of varying
93 garnet:clinopyroxene modal proportion considered representative of bulk-rock modal variance.
94 To retain textural information during subsequent laser-ablation (LA)-ICP-MS and SIMS
95 analyses, garnets were extracted from a number of distinct zones in this xenolith slice using a 2.5
96 mm diamond-coated steel core drill prior to mounting in the central portion of a 25 mm epoxy
97 mount.

98 **2.2 *In situ* major– and trace-element characterisation**

99 All mineral major-, minor-, and trace-element abundances are reported in the
100 **supplementary materials** along with images of the studied sample regions. Mineral major-
101 element oxide abundances were determined by electron microprobe (EMP) analyses with a five
102 spectrometer Cameca SX-100 at the University of Alberta. All data were collected with a
103 focused (1 μm) 20 nA beam operating at 15 kV. Counting times for all elements were 20 to 30 s,
104 and standard PAP corrections were applied to all analyses using the software of Armstrong
105 (1995). Natural and synthetic standards were measured at intervals during each analytical

session to assess precision and accuracy. Element concentrations were always within 1 % of accepted values. Detection limits (3σ above background) were typically ≤0.03 wt. % for Na_2O, MgO, CaO, NiO, and K_2O, ≤0.04 wt. % for Al_2O_3, SiO_2, TiO_2, FeO, and V_2O_3, and ≤0.05 wt. % for MnO, P_2O_5, and Cr_2O_3. Additional information pertaining to the EMP methodology is included in the **supplementary materials.**

Garnet trace-element abundances were obtained at the Geological Survey of Canada, Ottawa, using a Photon Machines Analyte 193 nm Ar-F excimer laser coupled to an Agilent 7700x quadrupole ICP-MS. Analyses were performed using a 10-16 Hz laser repetition rate at a photon fluence of 4.4-7.0 Jcm^{-2}. Data were acquired with a 43 to 69 μm spot-size for garnets, and a 52 μm spot for clinopyroxenes. Basaltic glass reference materials, USGS GSD-1G and GSE-1G were utilized as primary standards, with a selection of in-house garnets as secondary reference standards. Further analytical details are included in the **supplementary materials.**

2.3 Ion-probe oxygen isotope analyses

All oxygen isotope compositions are reported relative to the Vienna Standard Mean Ocean Water (VSMOW) standard. Where this can be described as:

$$\delta^{18}O_{VSMOW}\ (‰) = [[(^{18}O/^{16}O)_{sample}/(^{18}O/^{16}O)_{VSMOW}] -1]*1000].$$

For simplicity the VSMOW subscript is omitted and $\delta^{18}O$ notation is used in the text herein.

Oxygen isotope compositions of garnets were determined *in situ* with a Cameca IMS-1280 ion microprobe at the Canadian Centre for Isotopic Microanalyses (CCIM) at the University of Alberta following procedures described by Ickert and Stern (2013). Calibration of the matrix correction, as described by Ickert and Stern (2013; cf. Page *et al.*, 2010), was conducted by

analysing a full suite of garnet working standards on a separate grain mount prior to analysing the samples in this study. Seven 2.5 mm diameter cores of eclogite were mounted in a single 25 mm epoxy grain mount along with several chips of working standard UAG and secondary standard S0088 (a Gore Mountain pyrope-almandine megacryst, and a Jeffrey Mine grossular, respectively). All rock chips and garnets were within 0.5 cm of the centre of the grain mount. Analyses were conducted in a single analytical session, using a 2.5-3.0 nA Cs primary beam with a 15 µm spot diameter. Thirty analyses of UAG were interspersed at regular intervals among 94 sample points and seven analyses of S0088 (treated as an 'unknown') were collected during the analytical session for quality assurance. This yielded an S0088 average δ^{18}O-value of 4.13 ± 0.09 ‰ (2σ), n = 7, which coincides with the mean reported in an independent study conducted by Ickert and Stern (2013), indicating that the matrix correction is accurate. Total propagated uncertainties (including calibration uncertainty) on each analytical point are ±0.2-0.3 ‰ (2σ). All data are reported in the **supplementary materials**.

3. Results

3.1 Petrographic characteristics

In 09RV09, garnet-rich, and clinopyroxene-rich zones are unevenly distributed across the ~23 cm^2 surface area studied (**Fig. 2**). Larger (up to 5 mm in maximum dimension) garnet and clinopyroxene crystals, with well-developed lamellar pyroxene, and garnet exsolution, respectively, account for ~5-10 % of the studied eclogite surface. These large clinopyroxene crystals are turbid in appearance and generally exhibit narrow (<750 µm) sponge-textured rims texturally analogous to those reported for some Bellsbank eclogites (e.g., Taylor and Neal, 1989). The remaining surface area is dominated by rounded interlocking grains (generally 2-3

mm in maximum dimension) of garnet and clinopyroxene. Minor interstitial phases include phlogopite (up to 1 mm in maximum dimension), sulphide (generally < 500 μm maximum dimension), graphite (<650 μm), diamond (up to 800 μm in the studied portions of 09RV09), and anhedral clinopyroxene (generally <700 μm). Narrow veins (<150 μm) and cracks (<10 μm) on grain boundaries and penetrating larger crystals contain trapped melt (~60-80 vol. %) with lesser amounts of K-rich phlogopite (≤50 μm), clinopyroxene (≤20 μm), and small needles of Ti-oxide and sulphide (<1 μm wide, up to 8 μm in length). Utilising the textural classification of MacGregor and Carter (1970), the sample is a Group I eclogite. Notably, other accessory mineral phases, for example apatite ± magnesite ± monazite ± kyanite ± coesite ± dolomite, which have been observed in other eclogite xenoliths (Sobolev *et al.*, 1994; Snyder *et al.*, 1998) and carbonated high-pressure experimental assemblages (Knoche *et al.*, 1999; Dasgupta *et al.*, 2004) are absent from the studied sample.

Zones rich in garnet have garnet-clinopyroxene ratios of ~90:10 to ~70:30, whereas clinopyroxene-rich zones have garnet-clinopyroxene ratios of ~10:90 to ~30:70. Petrographic study and X-ray tomography (**supplementary materials**) show that abundances and spatial distributions of accessory phlogopite, sulphide, and diamond are not directly correlated with one another, and these do not vary in a systematic manner with garnet and clinopyroxene modal abundances.

3.2 Mineral major- and trace-element abundances

In situ mineral major- and trace-element abundances of 09RV09 are reported in the **supplementary materials** where reasoning for the use of the geometric form of trace-element anomalies throughout this text is discussed. Clinopyroxenes are characterised by Mg# values of

171 86.6-90.0 (where Mg# = 100Mg/[Mg+Fe^{total}]) and jadeite contents that generally range from 13-
172 24 mol. %. Clinopyroxene TiO_2 abundances range from 0.16-0.29 wt. %, Cr_2O_3 contents vary
173 from <0.05-0.21 wt. %, and K_2O concentrations are generally 0.18-0.29 wt. %, with only two
174 data points at sponge-textured clinopyroxene rims recording <0.04 wt. % K_2O. These
175 clinopyroxene compositions are broadly similar to those reported for other diamondiferous and
176 textural Group I eclogites (e.g., Jacob, 2004; Smart *et al.*, 2009).

177 Garnet compositions show small to moderate intra- and inter-grain major-element variation
178 with Mg# of 75.8 to 79.2 and Ca# of 8.2 to 10.4 (where Ca# = 100Ca/[Ca+Mg+Fe^{total}]), with no
179 consistent trend observed in core to rim traverses. These garnets have low Cr_2O_3 contents (≤0.25
180 wt. %), low Cr# values (< 0.70, where Cr# = 100Cr/[Cr+Al]), combined FeO^{total} + CaO contents
181 of 13.0-16.6 wt. %, and Na_2O contents ≤0.10 wt. %. This range of garnet major-element
182 compositions (**Fig. 3a-b**) overlaps that reported for textural Group I and Group II eclogites (±
183 diamond; McCandless and Gurney, 1989). Garnet compositions of 09RV09 are broadly
184 consistent with the Group-A garnet major-element classification of Taylor and Neal (1989).

185 Despite significant modal mineral variation, the silicate major-element characteristics of
186 09RV09 do not record the type of systematic mineral compositional variations found to
187 accompany variations in garnet-clinopyroxene proportions in some other modally variable
188 Roberts Victor eclogites. For instance, a diamondiferous eclogite xenolith containing exsolved
189 spinel (< 200 μm; RVSA-71, Ishikawa *et al.*, 2008a-b) and a diamondiferous spinel-free eclogite
190 (HRV-247; Hatton, 1978; O'Reilly and Griffin, 1995; Ishikawa *et al*. 2008a) showed variations
191 in clinopyroxene jadeite contents, and grossular proportions in garnet that were lower in
192 clinopyroxene-rich zones while the Mg# of both of these phases was lower in garnet-rich zones.

193 Chondrite normalised rare-earth-element (REE) abundances of 09RV09 garnets are LREE-
194 depleted relative to HREE ($[La/Yb]_N$ = 0.001-0.019, where N denotes normalisation to CI-
195 chondrite; **Fig. 4a**). Primitive mantle normalised trace-element abundance patterns (**Fig. 4b**)
196 display negative Sr- and Ti-anomalies (generally 0.10-0.40 and 0.27-0.47, respectively). In
197 detail, 09RV09 garnets show moderate variations in LREE abundances (e.g., La = 6-70 ppb), Ti,
198 and Hf (88-1386 ppm, and 70-900 ppb, respectively), but little to no variation beyond analytical
199 uncertainties in HREE, Y, Sc, V, and Zr contents (**supplementary materials**). Abundances of
200 Ti and Hf do not co-vary with La, and La abundances in excess of 20 ppb are restricted to three
201 data points for a single grain distal from zones with the most extreme garnet:clinopyroxene
202 values. The time-resolved ablation signals for these data points do not show resolvable inclusion
203 signals and these La contents are, therefore, considered to represent either a combination of
204 volumetrically minor, finely-disseminated, and evenly distributed LREE-enriched inclusions in
205 the sampled volume, or higher LREE abundances truly intrinsic to this grain. Notably, all
206 09RV09 garnet data points are characterised by little to no Eu-anomaly beyond analytical
207 uncertainties ($[Eu/Eu^*]_N$ = 1.0-1.4 and relative errors of 9-21 %, 2σ).

208 In contrast to garnet, all 09RV09 clinopyroxene analyses are LREE-enriched ($[La/Yb]_N$ =
209 8.52-29.2). These clinopyroxenes lack detectable Eu-anomalies, have positive Sr-anomalies
210 (2.4-4.7), negative Ti-anomalies (0.24-0.42; **Fig. 4b**), and are generally characterised by positive
211 $[Zr/Hf]_{PM}$ values (0.50-0.70) and Ti, V and Sc abundances show little or no variation beyond
212 analytical uncertainties. Detectable variations are present in clinopyroxene LREE, MREE
213 HREE, Y, Sr, Zr, Hf, Nb, and Ta abundances; of these the LREE strongly correlate with one
214 another and HFSE are strongly or very strongly correlated (e.g., **supplementary materials**).
215 However, comparison of clinopyroxene LREE, Sr, and HFSE abundances shows that these

element groups, and Sr, do not co-vary as high degrees of scatter are evident ($R^2 \leq 0.3$). Correlations of LREE with MREE, Y, and HREE are moderate to weak, and uncertainties on MREE, HREE, and Y abundances limit confident interpretations of these relationships. Significantly, no strong correlations are evident when abundances of LREE, Sr, Zr, Hf, Nb, and Ta in clinopyroxene are compared with La contents of texturally associated garnet (not plotted here).

The range of garnet and clinopyroxene trace-element abundances and inter-element fractionations determined for 09RV09 are broadly analogous to those reported for other Mg-rich eclogites (e.g., Barth *et al.*, 2002; Smart *et al.*, 2009). Gréau *et al.* (2011) suggested that clinopyroxene trace-element criteria differ between textural Group I and Group II eclogites thereby extending the earlier classification scheme of McCandless and Gurney (1989); comparison with recently recommended discrimination criteria shows that 09RV09 clinopyroxene Zr abundances are consistent with the Group I classification of Gréau *et al* (2011). On the other hand, Sr and Nd contents of 09RV09 clinopyroxene (472-835 ppm, 7.2-14 ppm, respectively) are higher than other Group I eclogites, and corresponding Ti and Zr abundances vary over a range (with associated uncertainties) that overlaps both Group I and Group II characteristics of Gréau *et al.*, (2011). This chemical variability undermines a simple classification scheme based on trace-elements but also emphasises the suitability of sample 09RV09 for studying the effects of metasomatic processes on oxygen isotope compositions. Critically, garnets and clinopyroxenes of 09RV09 do not exhibit systematic variations in the trace-element abundances determined for regions with differing garnet:clinopyroxene modal proportions, and abundances and inter-element ratios of trace-elements, which cover a wide-

range of geochemical properties, do not correlate systematically with major-element concentrations, Mg#, and/or garnet grossular contents (e.g., **Fig. 5a**).

3.3 Garnet oxygen-isotope compositions

In situ oxygen isotope compositions of 94 analytical points in 7 garnets derived from texturally distinct locations in 09RV09 yield δ^{18}O-values of +6.2-6.8 ‰ with no detectable variation outside total analytical uncertainties. The mean, mode, and median of these garnet oxygen isotope compositions are coincident at +6.5 ‰ (**Fig. 6a**). The garnet δ^{18}O-values show negligible variations, while some major- and trace-element contents vary moderately. However, there is no systematic correlation between garnet oxygen isotope compositions and major-, and trace-element characteristics of 09RV09 garnets and clinopyroxenes at scales ranging from 10's µm to many cm (**supplementary materials**).

The probability of the mean garnet δ^{18}O-value of 09RV09 being equal to that of the mean of the mantle garnet δ^{18}O-distribution is low. Results of t-tests to compare 09RV09 garnet δ^{18}O-data with that of Mattey *et al.*, (1994) assuming garnet fractionation factors of <0.5 ‰ for olivine, orthopyroxene, and clinopyroxene, yield a very low probability (p <0.001) of coincident means in all cases (where t-tests include; 1) the Shapiro-Wilk approach that assumes both datasets are derived from normally distributed populations; and, 2) non-parametric Kolmogorov-Smirnov tests, including the Lilliefors correction, with assumptions of both equal and unequal variances applied during each t-test). In addition, Mann-Whitney Rank sum tests of these data also show that the mean of our garnet δ^{18}O-data is significantly different from garnet-equilibrium values calculated for mantle mineral laser-fluorination data reported by Mattey *et al*. 1994 (p <0.001).

4. Discussion

Constraining the origin of mantle eclogite xenoliths is of fundamental importance to studies of craton origin and evolution. Isotopic compositions (O, Mg, Pb-Pb, Sm-Nd, Lu-Hf, and Re-Os) reported for a number of diamondiferous and non-diamondiferous eclogite xenoliths of the Roberts Victor kimberlite suggest that these materials are derived from Archean subducted crust (e.g., Kramers, 1979; McGregor and Manton, 1986; Pearson *et al*, 1995; Shirey *et al.*, 2001; Jacob *et al.*, 2005; Wang *et al*., 2012). A recent study of mineral major- and trace-element characteristics and garnet δ^{18}O-compositions of 33 eclogite xenoliths from the Roberts Victor Mine (Gréau *et al.*, 2011), and an investigation of a single texturally complex eclogite (RV07-17; Huang *et al*., 2014), have questioned the robust nature of garnet δ^{18}O-values as tracers of a crustal precursor for eclogites; these authors suggested that oxygen isotopes are markedly fractionated by mantle metasomatic processes. In particular, Gréau *et al.* (2011) suggested that garnet δ^{18}O-values are correlated with clinopyroxene incompatible element abundances, arguing that garnet oxygen isotope compositions reflect carbonatite metasomatism. Our detailed investigation of 09RV09 provides an important data-set to evaluate the robustness of garnet oxygen isotope compositions to metasomatic processes.

4.1 Metasomatic modification of 09RV09

Metasomatic modification of 09RV09 is evident in the form of late-stage infiltration along garnet and clinopyroxene grain boundaries (generally <150 μm wide) and narrow cracks (<10 μm) penetrating coarse-sized (2-3mm) garnets and clinopyoxenes. These narrow features contain trapped melt (~60-80 vol. % of the infiltration zones) with lesser amounts of K-rich phlogopite (≤50 μm), clinopyroxene (≤20 μm), and small needles of Ti-oxide and sulphide (<1

μm wide, up to 8 μm in length) and are interpreted as metasomatic in origin. In some cases, needle-like phases (<5μm in length) have nucleated at the grain boundaries of large, pre-existing, garnet and clinopyroxene and have grown outwards into narrow infiltration zones (**Fig. 7a**). Larger phlogopite grains (up to 500 μm) in 09RV09 generally occur at the point where several narrow (<1 mm wide) infiltration zones connect to one another. Though textural observations alone make it difficult to fully assess the genetic origin of these phases, we consider large phlogopites as crystals formed during metasomatic infiltration experienced by 09RV09; this interpretation is consistent with previous suggestions of a metasomatic origin for phlogopites of other Roberts Victor eclogite xenoliths (e.g., Ongley *et al.*, 1987). The relatively high K_2O contents (generally >0.20 wt. %) of 09RV09 clinopyroxenes are within the range reported for other textural Group I diamondiferous eclogite xenoliths (e.g., McCandless and Gurney, 1989) and eclogitic clinopyroxene inclusions in diamond (e.g., Taylor *et al.*, 1998, 2000; Stachel and Harris, 2008 and references therein). Previous studies (e.g., Hatton, 1978; Gréau *et al.*, 2011) have suggested that clinopyroxene K_2O contents above 0.07 wt. % are indicative of metasomatic modification associated with diamond formation in mantle environments, and these studies generally show elevated Na_2O contents (>0.09 wt. %) in garnet accompanying the high K concentrations in clinopyroxene (e.g., Hatton, 1978). Further, 09RV09 clinopyroxenes preserve notable inter- and intra-grain heterogeneity in the form of LREE, MREE, Sr, Ti and Nb abundances. In contrast, 09RV09 garnets are generally characterised by intra-grain major- and trace-element homogeneity and generally have Na_2O contents <0.09 wt. %. These garnets have higher Ti abundances compared with some - not all - textural Group II eclogites (**supplementary materials**), but lower Ti contents than mean and median values of eclogitic garnet diamond inclusions (e.g., Stachel and Harris, 2008).

The number of diamonds (>100 μm) observed *in situ* is small (n = 7), but those identified occur in regions of intersecting infiltration zones (± adjacent phlogopite). The uneven distribution of 09RV09 diamonds, and their occurrence in interstitial regions, is consistent with observations reported for other diamondiferous eclogite xenoliths (e.g., Anand *et al.*, 2004; Spetsius and Taylor, 2008). However, the clear evidence for metasomatic modification of 09RV09 makes it imperative that potential evidence of the protolith is treated cautiously.

4.1.1 Element exchange processes at the grain-scale

The disparate degree of equilibration exhibited by 09RV09 clinopyroxenes and garnets testifies to differing element exchange behaviours in these phases (cf., Burton *et al.*, 1995; Taylor *et al.*, 1996) with respect to the metasomatic history of this sample. An end-member model developed here specifically for 09RV09 references theories of diamond formation and takes account of regional tectonomagmatic events likely to have affected materials in proximity to the Colesburg Lineament, and sampled by the Cretaceous Roberts Victor kimberlite proximal to that major intra-cratonic terrane boundary (**Fig. 1**). Our model involves two metasomatic events influencing a garnet-clinopyroxene protolith after incorporation into the lithospheric mantle; the first being ancient and involving metasomatism at great depth by carbon-bearing fluids facilitating diamond formation broadly synchronous with stabilisation of the Kaapvaal Craton >2.5 Ga (see Pearson and Wittig, 2008; Helmstaedt *et al.*, 2010; Shu and Brey, 2015) and potentially concurrent with suturing along the Colesburg Lineament at ~2.9 Ga (Schmitz *et al.*, 2004; Shu *et al.*, 2013). This ancient metasomatism is followed by elemental and isotopic equilibration of silicate phases during protracted high-pressure, high-temperature residence in lithospheric mantle. Magnesium may be introduced during ancient metasomatism, and/or a small degree of melt removal may be facilitated by fluid introduction (where melt removal is

anticipated to cause only a small shift to lower δ^{18}O-values; Williams *et al.*, 2009). Thus, the relatively magnesian nature of this sample and the homogenous but higher Mg# of garnet in close proximity to diamond (**Fig. 3b**) may be, at least in part, related to an ancient metasomatic event. The second modification event in our model scenario involves a late-stage metasomatic interaction linked to kimberlite arrival and xenolith entrainment at ~124 Ma (Smith *et al.*, 1985) contributing to frozen records of inter-and intra-grain heterogeneity in 09RV09 clinopyroxenes. Assessing the validity of this model requires consideration of the nature of element exchange in eclogitic garnets and omphacitic pyroxenes (**supplementary materials**). For example, the intra-grain homogeneity displayed by 09RV09 garnets may reflect relatively fast element exchange and equilibration of major- and trace-element abundances in garnet during a single metasomatic event when compared with co-existing clinopyroxene. Alternatively, element exchange processes in garnet may be orders of magnitude slower than those operating in clinopyroxene leading to the conclusion that the garnets retain robust records of their mantle protolith that are resistant to late-stage small-volume metasomatic modification.

Equilibration temperatures calculated for clinopyroxene cores and coexisting garnets in 09RV09 are within the range anticipated for cratonic lithospheric mantle materials resident at depths in which diamond is stable. Given this observation, we reason that 09RV09 garnet compositions reflect equilibrated mantle compositions minimally disturbed by late-stage small-volume metasomatism. In contrast, trivalent LREE-MREE, tetravalent HFSE, and divalent cations of small ionic radius (e.g, Fe, Mg, Mn) may have diffused relatively rapidly in the outer portions of 09RV09 clinopyroxenes as a result of recent metasomatic disturbance. The observed decoupling between REE and HFSE in 09RV09 clinpyroxenes likely relate to differences in the rate or nature of REE and HFSE element exchange in clinopyroxene, potentially high HFSE

blocking temperatures, and/or sequestering of HFSE by volumetrically minor rutile needles crystallised in corresponding metasomatic infiltration zones. It is likely that all of these factors contributed during metasomatic modification of 09RV09 clinopyroxenes.

4.1.2 Bulk-rock reconstruction and its constraints on 09RV09 metasomatism

The precise nature of fluids that infiltrated 09RV09, related to diamond formation, and kimberlite entrainment, is not well constrained at this time (e.g., speciation, fO_2, isotopic characteristics). Given the similarities between 09RV09 silicate trace-element characteristics and those of silicate diamond inclusion data (e.g., Ireland *et al.*, 1994; Taylor *et al.*, 1996, 2000; Sobolev *et al.*, 1998; Stachel *et al.*, 2004), metasomatic agents that have influenced 09RV09 likely resemble the spectrum of compositions reported for diamond fluid inclusions. For these reasons, we model the trace-element composition resulting from mixing between possible protolith compositions and anticipated metasomatic fluids. Modification by kimberlite (generally considered to be CO_2-rich and LREE-enriched; e.g., Becker and Le Roux, 2006; Kjarsgaard *et al.*, 2009) and/or potential LREE-enriched fluids derived from the host kimberlite is possible, but is considered to be volumetrically minor.

Bulk-rock reconstructions utilise representative garnet and clinopyroxene trace-element core compositions, trace-element characteristics of altered gabbro (e.g., Hart *et al.*, 1999; Bach *et al.*, 2001) previously considered by others as a possible eclogite protolith (e.g., Green and Ringwood, 1967), and trace-element compositions reported for gem-quality diamond (McNeill *et al.*, 2009) and fluid inclusions of fibrous diamonds (Klein-BenDavid *et al.*, 2010). Results of these calculations indicate that the addition of <<0.03 wt. % of a diamond-forming incompatible-element-rich fluid to an oceanic crustal protolith can account for the LREE-enrichment

calculated for the reconstructed bulk-rock compositions of 09RV09 (**Fig. 7b** and **supplementary materials**). The addition of similarly low metasomatic fluid proportions (<<0.05 wt. %) is required if the potential crustal protolith is considered to be derived from a more magnesian (relative to typical gabbro) sheeted dyke complex lacking Eu-anomalies (not shown) and/or an altered basalt of broadly picritic/komatiitic composition (cf., Shirey *et al.*, 2001). Given this evidence for metasomatic modification of 09RV09, we appraise the consequences for our interpretation of the homogeneous garnet δ^{18}O-compositions in this xenolith.

4.2 Oxygen-isotope signatures: metasomatism versus precursor inheritance

In contrast to the prevailing paradigm, it has been suggested that eclogite garnet oxygen isotope compositions in excess of the typical garnet mantle range may reflect secondary overprinting by the passage of carbonatitic melt (e.g., Gréau *et al.*, 2011), and/or could reflect interaction with CO-, OH, and/or CO_2-bearing fluids (e.g., Deines *et al.*, 1991) similar to those reported for diamond inclusions (e.g., Navon *et al.*, 1988; Turner *et al.*, 1990; Izraeli *et al.*, 2001; Klein-BenDavid, 2004, 2007; Tomlinson *et al.*, 2006) and observed in some mantle xenoliths transported by alkali basalts (e.g., Bergman and Dubessy, 1984; Andersen and Neumann, 2001). There are no oxygen isotopic determinations on primary carbonatites erupted in an un-modified state from the mantle with which to test this conjecture. Current experimental, empirical, and theoretical partition coefficients combined with fractionation factors reported for basaltic liquids and associated phases at temperatures of ~1000-1300ºC (cf., Eiler, 2001 and Chacko *et al.*, 2001) indicate that silicate δ^{18}O-values vary by <0.5 ‰ during the generation and fractional crystallisation of basaltic melts at high-temperatures (1000-1300ºC). In addition, pressure effects on isotopic exchange at crustal and upper-mantle conditions are thought to be small due to limited volume changes (<0.005 ‰ for pressure differences of 20-30 kbar; e.g., Clayton *et al.*,

1975; Polyakov and Kharlashina, 1994). Glass, CO, OH, and CO_2 species may fractionate $\delta^{18}O$-compositions by detectable amounts (>>0.5 ‰; Deines *et al.*, 1991), but the effect of possible solutes, and their potential speciation variations, on oxygen isotope fractionation in mantle fluids carrying gaseous molecules is not well constrained at conditions appropriate for mantle environments (e.g., O'Neil, 1986; Bindeman, 2008 and references therein). Zheng (1993) suggested that, under certain circumstances, partial substitution of $[OH]_4^{-4}$ for $[SiO_4]^{-4}$ in grossular molecules could potentially lead to ^{18}O-enrichment, and Kohn and Valley (1998) proposed that octahedral cation substitutions may also influence garnet $\delta^{18}O$-values. Oxygen diffuses slowly in garnet even under hydrous conditions (e.g., Lichtenstein and Hoernes, 1992; Cole and Chakraborty, 2001). For these reasons, and considering mass-balance requirements, kinetic processes such as diffusion, and/or solution-precipitation, associated with metasomatic exchange in mantle environments will potentially lead to disequilibrium characteristics in the form of garnet compositional zoning developed during complex multi-stage histories (e.g., Zhang *et al.*, 2000) anticipated for SCLM residence times up to Gyrs.

Given the complex metasomatic history of sample 09RV09 we might expect to see some measureable small-scale variations in oxygen isotope compositions that, for instance, relate to elemental or textural variation. No variation in garnet $\delta^{18}O$-values exists. The data are within measurement uncertainty both within garnet grains and in garnets across the entire xenolith. Similarly, garnets in a coesite-rutile-bearing eclogite from Roberts Victor with abundant veinlets (sample 13-64-136), also lack inter- and intra-grain variation in garnet $\delta^{18}O$-compositions (Russell *et al.*, 2013). These observations contrast to inter-sample garnet $\delta^{18}O$ variance reported for a texturally complex eclogite (RV07-17; Huang *et al.*, 2014). Moreover, there is no correlation at all between clinopyroxene incompatible element abundances such as La and garnet

δ^{18}O-values for 09RV09 (**Fig. 5b**), indicating that incompatible-element enrichment due to metasomatism is unlikely to be the primary control on the oxygen isotopic composition of this eclogite. This result means that a metasomatic origin of the statistically non-robust correlation between La and δ^{18}O-values presented by Gréau *et al.* (2010; **Fig. 5b**) is unlikely ($p<0.001$). No valid mixing curve is evident in the combined data set, especially considering that the Group II eclogites included in the Gréau *et al.* (2010) are part of a separate group of eclogites from Roberts Victor whose δ^{18}O-values range to above +6 ‰; e.g., Ongley *et al.*, 1987). This consideration weakens the argument for metasomatic overprinting of garnet δ^{18}O-compositions and hence the existing and new eclogite data plotted on this co-variation diagram, therefore, is not able to provide a unique solution to account for eclogitic garnet δ^{18}O-compositions.

Mass balance considerations with respect to garnet oxygen isotope compositions (where oxygen is a major-element) offer a more powerful argument in that to significantly modify the oxygen isotopic composition over 1 ‰ away from the canonical mantle value requires equilibration with substantially larger relative volumes of fluid (or unrealistic δ^{18}O-compositions) than can be accounted for by the degree of trace-element modification in 09RV09. A metasomatic model postulated to drive volumetrically significant ^{18}O enrichments (or depletions) in eclogite garnet δ^{18}O-compositions requires that a highly reactive, volatile-rich agent traverse substantial quantities of mantle without equilibrating with the ambient material. Mass balance ("closed system") and Rayleigh ("open system") models (e.g., **Fig. 8;** Taylor, 1977; Criss and Taylor, 1986) place constraints on the degree of fluid-rock interaction required to buffer a fluid with an initial δ^{18}O-value of +7.5 ‰. In these models, we utilised forsterite-calcite and calcite-CO_2 oxygen isotope fractionation factors (yielding ΔCO_2-forsterite = +4.1 ‰; Chiba et al., 1989; Chacko et al., 1991) and a calcite-H_2O fractionation factor (giving ΔH_2O-

forsterite = +0.3 ‰; O'Neil et al., 1969; Friedman and O'Neil, 1977). At an assumed temperature of 1100 °C, a closed-system model predicts that 1 g of a fluid, rich in H_2O or CO_2, requires 15-20 grams of peridotite (approximated by forsterite = +5.0 ‰) to become buffered to a composition within ±0.5 ‰ of the median peridotitic mantle value. Under open-system conditions, which may provide a more realistic analogue for mantle metasomatism, fluid interaction with substantially less peridotite for a given fluid volume (<1:5 fluid-rock ratio) is required to buffer the fluid $\delta^{18}O$-value to the composition of silicate mantle with which it is interacting. These models show that only minor fluid-rock interaction is required to buffer the oxygen isotope composition of a mantle metasomatic fluid. To generate the 09RV09 garnet $\delta^{18}O$-value of +1 ‰ above the mantle value, and up to +3.5 ‰ observed in other eclogites, mantle pyroxenites and diamond inclusions (MacGregor and Manton, 1986; Pearson *et al.*, 1991; Jacob *et al.*, 2003; Ickert *et al.*, 2015) requires not only that very high fluid-rock ratios (≥2:5; **Fig. 8**) are maintained for a compositionally extreme fluid at the local "sample scale" but that these extreme $\delta^{18}O$-compositions are continuously maintained from the fluid source, throughout its flow at great depth (asthenospheric and/or lithospheric mantle), where the fluid flow regime is likely percolative. Therefore, the probability of a metasomatic fluid with an extreme oxygen isotope composition surviving unmodified during transport through the mantle, itself dominantly peridotitic, and imposing this signature on an eclogite body within the peridotite is very low indeed. This clearly favours the interpretation of 09RV09 garnet $\delta^{18}O$-values as representing a robust tracer of the protolith lithology rather than the product of mantle metasomatism.

Evaluating the suggestion that diamond-forming fluids in general may be responsible for generating exotic mantle oxygen isotopic compositions (Gréau *et al.* 2011) we note that 6 peridotite suite garnets included in diamonds analysed by Mattey *et al.* (1994) have a mean $\delta^{18}O$-

value of +5.3 ‰, identical to typical mantle peridotite. Hence, there is no solid evidence for appreciable oxygen isotope modification in garnet-bearing mantle materials during metasomatism by small-volume incompatible-element enriched fluids. Indeed, it is more likely that δ^{18}O-compositions of small-degree metasomatic fluids equilibrate with the host rock and, thus, we reason that mantle eclogites and peridotites impart their oxygen isotope signature on volumetrically minor and transient fluids during metasomatism and diamond evolution.

4.3 Summary and implications

To critically appraise the nature of potential metasomatic signatures in mantle eclogite xenoliths, we conducted a multi-technique *in situ* study of a diamondiferous eclogite xenolith with varying garnet:clinopyroxene proportions (09RV09) from the Roberts Victor kimberlite, S. Africa. We provided the first *in situ* measurements of δ^{18}O-values in eclogitic garnet in close proximity to diamond, and retaining textural control, to test theories concerned with metasomatic modification of eclogites during diamond formation, particularly garnet oxygen isotope compositions.

Intra-grain variations in clinopyroxene major-element, LREE-MREE and HFSE contents appear to have resulted from later metasomatism related to kimberlite arrival and xenolith entrainment, yet oxygen isotope compositions in garnet are uniform, within tight analytical uncertainties, across the xenolith in a wide variety of textural settings. SIMS garnet δ^{18}O-values of 6.5 ± 0.2 ‰ are higher than the mean mantle garnet range (4.8-5.5 ‰). There is no co-variation of oxygen isotope composition with incompatible element based indicators of metasomatism.

The lack of detectable inter- and intra-grain oxygen isotope variation in 09RV09 garnet, including garnet in close proximity to diamond, indicates that garnet δ^{18}O-compositions are ancient and likely not affect by infiltration of diamond-forming fluids. The intra-sample garnet oxygen isotope homogeneity of 09RV09 is of particular interest as available data suggest that intra-sample garnet oxygen isotope homogeneity is likely representative of mantle eclogites in general. Prior laser-fluorination (LF) studies of garnet separates have generally shown highly reproducible eclogite garnet δ^{18}O-compositions within a given sample both at individual laboratories and in inter-laboratory comparison studies (e.g., Rumble *et al.*, 2007). Furthermore, results of other recent *in situ* studies of garnet δ^{18}O-compositions of 52 other eclogite xenoliths have demonstrated intra-sample homogeneity (Russell *et al.*, 2013; Smit *et al.*, 2014; Dongre *et al.*, 2015) with only one known exception; RV07-17 (Huang *et al.*, 2014). Our data, combined with the slow time-scales of oxygen isotopic diffusion in the mantle (cf., Russell *et al.*, 2013) and the difficulties in moving metasomatic fluids with exotic oxygen isotopic compositions through the Earth's mantle without buffering their compositions to the mantle δ^{18}O-value support the concept that eclogite oxygen isotope compositions largely reflect their crustal precursors.

The oxygen isotope composition of garnets in 09RV09 is significantly different from typical mantle values supporting a crustal origin for its precursor and in line with many other studies of Roberts Victor eclogite xenoliths and eclogitic diamond inclusions (e.g., MacGregor and Manton, 1986; Jacob *et al.*, 2005; Tappert *et al.*, 2005; Schulze *et al.*, 2013; Ickert *et al.*, 2013, 2015), irrespective of their textural groupings.

5. Acknowledgements

Funding to DGP supported this research and was provided by the CERC programme. Sergei Matveev is thanked for his assistance during electron microprobe analyses. Three anonymous reviewers and the Associate Editor, Dmitri A. Ionov, are thanked for constructive suggestions that have helped to improve this manuscript.

7. References

Anand M., Taylor L. A., Misra K. C., Carlson W. D., and Sobolev N. V. (2004). Nature of diamonds in Yakutian eclogites: views from eclogite tomography and mineral inclusions in diamonds. *Lithos*, *77*(1), 333-348.

Andersen T., and Neumann E.R., 2001. Fluid inclusions in mantle xenoliths. *Lithos*, 55(1), 301-320.

Armstrong, J.T., (1995). A package of correction programs for the quantitative electron microbeam X-ray analysis of thick polished materials, thin films, and particles. *Microbeam Anal.*, 4, 177-200.

Aulbach S., Pearson N.J., O'Reilly S.Y., and Doyle B.J., 2007. Origins of xenolithic eclogites and pyroxenites from the Central Slave Craton, Canada. *J. Petrol.* 48, 1843–1873.

Bach W., Alt J.C., Niu Y., Humphris S.E., Erzinger J., and Dick H.J.B., 2001. The geochemical consequences of late-stage low-grade alteration of lower ocean crust at the SW Indian Ridge: results from ODP Hole 735B (Leg 176). *Geochim. Cosmochim. Acta.*, 65, 3267–3287.

Baker J., Matthews A., Mattey D., Rowley D., and Xue F., 1997. Fluid-rock interactions during ultra-high pressure metamorphism, Dabie Shan, China. *Geochim. Cosmochim Acta*, 61(8), 1685-1696.

Barth M.G., Rudnick R.L., Horn I., McDonough W.F., Spicuzza M.J., Valley J.W., and Haggerty S.E., 2001. Geochemistry of xenolithic eclogites from West Africa, part I: a link between low MgO eclogites and archean crust formation. *Geochim. Cosmochim. Acta*, 65 (9), 1499–1527.

Barth M.G., Rudnick R.L., Horn I., McDonough W.F., Spicuzza M.J., Valley J.W., and Haggerty S.E., 2002. Geochemistry of xenolithic eclogites from West Africa, part 2; Origins of the high MgO eclogites. *Geochim. et Cosmochim. Acta*, 66(24), 4325-4345.

Beard B.L., Fraracci K.N., Taylor L.A., Snyder G.A., Clayton R.A., Mayeda T.K., and Sobolev N.V., 1996. Petrography and geochemistry of eclogites from the Mir kimberlite, Yakutia, Russia. *Contrib. Mineral. Petrol.*, 125, 293-310.

Becker M., and Le Roex A. P., 2006. Geochemistry of South African on-and off-craton, Group I and Group II kimberlites: petrogenesis and source region evolution. *J. Petrol.*, 47(4), 673-703.

Bergman S.C., and Dubessy J., 1984. CO_2-CO fluid inclusions in a composite peridotite xenolith: implications for upper mantle oxygen fugacity. *Contrib. Mineral. Petrol.*, 85(1), 1-13.

Bindeman I., 2008. Oxygen isotopes in mantle and crustal magmas as revealed by single crystal analysis. *Rev. Mineral. Geochem.*, 69(1), 445-478.

Burton, K. W., Kohn, M. J., Cohen, A. S., and O'Nions, R. K., 1995. The relative diffusion of Pb, Nd, Sr and O in garnet. *Earth Planet. Sci. Lett.*, 133(1), 199-211.

542 Caporuscio F.A., 1990. Oxygen isotope systematics of eclogite mineral phases from South Africa. *Lithos*,
543 25, 203-210.

544 Carmody L., Barry P.H., Shervais J.W., Kluesner J.W., and Taylor L.A., 2013. Oxygen isotopes in
545 subducted oceanic crust: A new perspective from Siberian diamondiferous eclogites. Geochem.
546 Geophys. Geosyst., 14(9), doi: 10.1002/ggge.20220.

547 Chacko T., Cole D.R., and Horita J., 2001. Equilibrium oxygen, hydrogen and carbon isotope
548 fractionation factors applicable to geologic systems. *Rev. Mineral. Geochem.*, 43(1), 1-81.

549 Chacko T., Mayeda T. K., Clayton R. N., and Goldsmith J. R., 1991, Oxygen and carbon isotope
550 fractionations between CO_2 and calcite. *Geochim.Cosmochim. Acta*, 55(10), 2867-2882.

551 Chiba H., Chacko T., Clayton R. N., and Goldsmith J. R., 1989, Oxygen isotope fractionations involving
552 diopside, forsterite, magnetite, and calcite: Application to geothermometry. *Geochim. Cosmochim.*
553 *Acta*, 53(11), 2985-2995.

554 Clayton R.N., Goldsmith J.R., Karel K.J., Mayeda T K., and Robert C.N., 1975. Limits on the effect of
555 pressure on isotopic fractionation. *Geochim. Cosmochim. Acta*, 39(8), 1197-1201.

556 Cole D.R., and Chakraborty S., 2001. Rates and mechanisms of isotopic exchange. *Rev. Mineral.*
557 *Geochem.*, 43(1), 83-223.

558 Coleman R. G., Lee D. E., Beatty L. B., and Brannock W. W., 1965. Eclogites and eclogites: their
559 differences and similarities. *Geol. Soc. Am. Bullet.*, 76(5), 483-508.

560 Criss R. E., and Taylor Jr. H. P., 1986, Meteoric-hydrothermal systems. *Rev. Mineral.*, 16, 373-424.

561 Dasgupta R., Hirschmann M. M., and Withers A. C., 2004. Deep global cycling of carbon constrained by
562 the solidus of anhydrous, carbonated eclogite under upper mantle conditions. *Earth Planet. Sci. Lett.*,
563 *227*(1), 73-85.

564 Deines P., Harris J.W., Robinson, D.N., Gurney, J.J., and Shee, S.R., 1991. Carbon and oxygen isotope
565 variations in diamond and graphite eclogites from Orapa, Botswana, and the nitrogen content of their
566 diamonds. *Geochim.et Cosmochim. Acta*, 55(2), 515-524.

567 Dongre A. N., Jacob D. E., and Stern R. A., 2015. Subduction-related origin of eclogite xenoliths from
568 the Wajrakarur kimberlite field, Eastern Dharwar craton, Southern India: Constraints from petrology
569 and geochemistry. *Geochim. Cosmochim. Acta*, 166, 165-188.

570 Eiler J.M., 2001. Oxygen isotope variations of basaltic lavas and upper mantle rocks. *Rev. Mineral.*
571 *Geochem.*, 43(1), 319-364.

572 Friedman I., and O'Neil, J. R., 1977, Compilation of stable isotope fractionation factors of geochemical
573 interest. In *Data of Geochemistry 6th Ed.*, (Vol. 440). US Govt., Washington, USA.

574 Garlick G.D., MacGregor I.D., and Vogel D.E., 1971. Oxygen isotope ratios in eclogites from
575 kimberlites. *Science*, 172, 1025–1027.

576 Gréau Y., Huang J.-X., Griffin W.L., Renac C., Alard O., and O'Reilly S.Y., 2011. Type I eclogites from
577 Roberts Victor kimberlites: Products of extensive mantle metasomatism. *Geochim. Cosmochim. Acta*,
578 75, 6927-6954.

579 Green D. H., and Ringwood A. E., 1967. An experimental investigation of the gabbro to eclogite
580 transformation and its petrological applications. Geochimica et Cosmochimica Acta, 31(5), 767-833.

Gregory R.T., and Taylor Jr. H.P., 1981. An oxygen isotope profile in a section of Cretaceous oceanic crust, Samail ophiolite, Oman: Evidence for $\delta^{18}O$ buffering of the oceans by deep (>5 km) seawater-hydrothermal circulation at mid-ocean ridges. *J. Geophys Res*, 86(B4), 2737-2755.

Gurney, J. J., Helmstaedt, H. H., Richardson, S. H., and Shirey, S. B., 2010. Diamonds through time. *Econ. Geol.*, 105(3), 689-712.

Hart S.R., Blusztain J., Dick H.J.B., Meyer P.S., and Muehlenbachs K.,1999. The fingerprint of seawater circulation in a 500-meter section of ocean crust gabbros. *Geochim. Cosmochim. Acta.*, 63, 4059–4080.

Hatton C.J., 1978. The geochemistry and origin of xenoliths from the Roberts Victor Mine. *PhD thesis, Univ. Cape Town, Cape Town, South Africa.*

Hatton C.J., and Gurney J.J., 1987. Roberts Victor eclogites and their relation to the mantle. *In: Nixon P.H. (Ed.), Mantle Xenoliths, Wiley, Chichester*, pp. 453-463

Heaman L.M., Creaser R.A., and Cookenboo H.O., 2002. Extreme enrichment of high field strength elements in Jericho eclogite xenoliths: A cryptic record of Paleoproterozoic subduction, partial melting, and metasomatism beneath the Slave craton, Canada. *Geology*, *30*(6), 507-510.

Heaman L.M., Creaser R.A., Cookenboo H.O., and Chacko T., 2006. Multi-stage modification of the Northern Slave mantle lithosphere: evidence from zircon-and diamond-bearing eclogite xenoliths entrained in Jericho kimberlite, Canada. *J. Petrol.*, *47*(4), 821-858.

Helmstaedt H., and Doig, R., 1975. Eclogite nodules from kimberlite pipes of the Colorado Plateau – samples of subducted Franciscan-type oceanic lithosphere. *Phys. Chem. Earth*, 9, 95-111.

Helmstaedt, H. H., Gurney, J. J., and Richardson, S. H., 2010. Ages of cratonic diamond and lithosphere evolution: constraints on Precambrian tectonics and diamond exploration. *Can. Min.*, 48(6), 1385-1408.

Huang J.-X., Gréau Y., Griffin W.L., O'Reilly S.Y, and Pearson N.J., 2012. Multi-stage origin of Roberts Victor eclogites: Progressive metasomatism and its isotopic effects. *Lithos*, 142-143, 161-181.

Huang J.-X., Griffin W.L., Gréau Y., Pearson N.J., O'Reilly S.Y., Cliff J., and Martin L., 2014. Unmasking xenolithic eclogites: Progressive metasomatism of a key Roberts Victor sample. *Chem. Geol., 364*, 56-65.

Ickert R.B., and Stern R.A., 2013. Matrix corrections and error analysis in high-precision SIMS $^{18}O/^{16}O$ measurements of Ca-Mg-Fe garnet. *Geostand. Geoanal. Res.*, 37(4), 429-448.

Ickert R.B., Stachel T., Stern R. A., and Harris, J. W., 2013. Diamond from recycled crustal carbon documented by coupled $\delta^{18}O$-$\delta^{13}C$ measurements of diamonds and their inclusions. *Earth Planet. Sci. Lett.*, 364, 85-97.

Ireland T.R., Rudnick R.L., and Spetsius Z., 1994. Trace elements in diamond inclusions from eclogites reveal link to Archean granites. *Earth Planet. Sci. Lett.*, 128(3), 199-213.

Ishikawa A., Pearson D.G., Maruyama S., Cartigny P., Ketchum R.A., and Gurney J.J., 2008a. Compositional layering in a highly diamondiferous eclogite xenolith from the Roberts Victor kimberlite, South Africa and its implications for diamond genesis. *IX International Kimberlite Conf.*, Abst. No. 9IKC-A-00078.

Ishikawa A., Pearson D.G., Maruyama S., de Bruin D., and Gurney J.J., 2008b. Compositional variability of the Roberts Victor eclogites: evidence for mantle metasomatism involving diamond dissolution. *IX International Kimberlite Conf.*, Abst. No. 9IKC-A-00079.

Izraeli E.S., Harris J.W., and Navon O., 2001. Brine inclusions in diamonds: a new upper mantle fluid. *Earth Planet. Sci. Lett.*, 187(3), 323-332.

Jacob D., 2004. Nature and origin of eclogite xenoliths in kimberlites. *Lithos*, 77, 295–316.

Jacob D., and Jagoutz E., 1994. A diamond-graphite bearing eclogitic xenolith from Roberts Victor (South Africa): Indications for petrogenesis from Pb-, Nd-, and Sr-isotopes. *In: Meyer H.O.A., Leonardos O.H. (Eds), Kimberlites, Related Rocks, and Mantle Xenoliths. Companhia de Pesquisa de Recursos Minerais, Spec. Pub. vol. 1/A*, pp. 304-317.

Jacob D., and Foley S.F., 1999. Evidence for Archean ocean crust with low high field strength element signature from diamondiferous eclogite xenoliths. *Lithos*, 48, 317-336.

Jacob D., Jagoutz E., Lowry D., Mattey D., and Kudrjavtseva G., 1994. Diamondiferous eclogites from Siberia: remnants of Archean oceanic crust. *Geochim. Cosmochim. Acta*, 58(23), 5191-5207.

Jacob D.E., Schmickler B., and Schulze D.J., 2003. Trace element geochemistry of coesite-bearing eclogites from the Roberts Victor Kimberlite. *Lithos*, 71, 337-351.

Jacob D., Bizimis M., and Salters V.J.M., 2005. Lu-Hf and geochemical systematics of recycled ancient oceanic crust: evidence from Roberts Victor eclogites. *Contrib. Mineral. Petrol.*, 148(6), 707-720.

Jagoutz E., Dawson J.B., Hoernes S., Spettel B., and Wanke H., 1984. Anorthositic oceanic crust in the Archean Earth. *XV Lunar Planet. Sci. Conf.*, pp. 395-396.

Kjarsgaard B. A., Pearson D. G., Tappe S., Nowell G. M., and Dowall D. P., 2009. Geochemistry of hypabyssal kimberlites from Lac de Gras, Canada: comparisons to a global database and applications to the parent magma problem. *Lithos*, 112, 236-248.

Klein-BenDavid O., Izraeli E.S., Hauri E., and Navon O., 2004. Mantle fluid evolution—a tale of one diamond. *Lithos*, 77(1), 243-253.

Klein-BenDavid O., Izraeli E.S., Hauri E., and Navon O., 2007. Fluid inclusions in diamonds from the Diavik mine, Canada and the evolution of diamond-forming fluids. *Geochim.et Cosmochim. Acta*, 71(3), 723-744.

Klein-BenDavid O., Pearson D.G., Nowell G.M., Ottley C., McNeill J.C., and Cartigny P., 2010. Mixed fluid sources involved in diamond growth constrained by Sr–Nd–Pb–C–N isotopes and trace elements. *Earth Planet. Sci. Lett.*, 289(1), 123-133.

Knoche R., Sweeney R. J., and Luth R. W. (1999). Carbonation and decarbonation of eclogites: the role of garnet. *Contrib. Mineral. Petrol.*, *135*(4), 332-339.

Kohn M.J., and Valley J.W., 1998. Effects of cation substitutions in garnet and pyroxene on equilibrium oxygen isotope fractionations. *J. Meta. Geol.*, 16(5), 625-639.

Konrad-Schmolke M., Zack T., O'Brien P.J., and Jacob D.E., 2008. Combined thermodynamic and rare earth element modelling of garnet growth during subduction: Examples from ultrahigh-pressure eclogite of the Western Gneiss Region, Norway. *Earth Planet. Sci. Lett.*, 272(1), 488-498.

Kramers J.D., 1979. Lead, uranium, strontium , potassium and rubidium in inclusion-bearing diamonds and mantle-derived xenoliths from southern Africa, *Earth Planet. Sci. Lett.*, 42, 58-70.

MacGregor I.D., and Carter J.L., 1970. The chemistry of clinopyroxenes and garnets of eclogite and peridotite xenoliths from the Roberts Victor Mine, South Africa. *Phys. Earth Planet. Interiors*, 3, 391-397.

MacGregor I.D., and Manton W.I., 1986. Roberts Victor Eclogites: Ancient Oceanic Crust. *J. Geophys. Res.*, 91(B14), 14,063-14,079.

Mattey D., Lowry D., and Macpherson C. (1994). Oxygen isotope composition of mantle peridotite. *Earth Planet. Sci. Lett.*, *128*(3), 231-241.

McCandless T.E., and Gurney J.J., 1989. Sodium in garnet and potassium in clinopyroxene; criteria for classifying mantle eclogites. *In: Ross J, (Ed) Kimberlites and related rocks. Their mantle/crustal setting, diamonds and diamond exploration*, vol. 2, Blackwell, Carlton, Australia, pp. 827-832.

McNeill J., Pearson D.G., Klein-BenDavid O., Nowell G.M., Ottley C.J., and Chinn I., 2009. Quantitative analysis of trace element concentrations in some gem-quality diamonds. *J. Phys.Cond. Matt.*, 21(36), 364207.

Navon O., Hutcheon I.D., Rossman G.R., and Wasserburg G.J., 1988. Mantle-derived fluids in diamond micro-inclusions. *Nature*, 355, 784-789.

Neal C.R., and Taylor L.A., 1990. Comment on "Mantle eclogites: evidence of igneous fractionation in the mantle" by J.R Smyth, F.A. Caporuscio, and T.C. McCormick. *Earth Planet. Sci. Lett.*, 101, 112-119.

Neal C.R., Taylor L.A., Davidson J.P., Holden P., Halliday A.N., Nixon P.H., Paces J.B., Clayton R.N., and Mayeda T.K., 1990. Eclogites with oceanic crustal and mantle signatures from the Bellsbank kimberlite, South Africa, part 2: Sr, Nd, and O isotope geochemistry. *Earth Planet. Sci. Lett.*, 99, 362-379.

O'Neil J. R., 1986. Theoretical and experimental aspects of isotopic fractionation. *Rev. Mineral. Geochem.*, 16(1), 1-40.

O'Neil J. R., Clayton R. N., and Mayeda T. K., 1969. Oxygen isotope fractionation in divalent metal carbonates. *J. Chem. Phys.*, 51, 5547-5558.

O'Reilly S.Y., and Griffin W.F., 1995. Trace-element partitioning between garnet and clinopyroxene in mantle-derived pyroxenites and eclogites: P-T-X controls. *Chem. Geol.*, 121(1-4), 105-130.

Ongley J.S., Basu A.R., and Kyser T.K., 1987. Oxygen isotopes in coexisting garnets, clinopyroxenes and phlogopites of Roberts Victor eclogites: implications for petrogenesis and mantle metasomatism. *Earth Planet. Sci. Lett.*, 83, 80-84.

Page F.S., Kita N. T., and Valley J.W., 2010. Ion microprobe analyses of oxygen isotopes in garnets of complex chemistry. *Chem. Geol.*, 270, 9-19.

Pearson D. G., and Wittig N., 2008. Formation of Archaean continental lithosphere and its diamonds: the root of the problem. *J.Geol. Soc.*, 165(5), 895-914.

Pearson D. G., Davies G. R., Nixon P. H., Greenwood P. B., and Mattey D. P. 1991, Oxygen isotope evidence for the origin of pyroxenites in the Beni Bousera peridotite massif, North Morocco: derivation from subducted oceanic lithosphere. *Earth Planet. Sci. Lett.*, 102(3), 289-301.

Pearson D. G., Snyder G. A., Shirey S. B., Taylor L. A., Carlson R. W., and Sobolev N. V., 1995. Archaean Re–Os age for Siberian eclogites and constraints on Archaean tectonics. *Nature*, *374*(6524), 711-713.

Pernet-Fisher J.F., Howarth G.H., Liu Y., Barry P.H., Carmody L., Valley J.W., Bodnar R.J., Spetsius Z.V., and Taylor L. A., 2014. Komsomolskaya diamondiferous eclogites: evidence for oceanic crustal protoliths. *Contrib. Min. Petro.*, *167*(3), 1-17.

Polyakov V.B., and Kharlashina N.N.,1995. The use of heat capacity data to calculate carbon isotope fractionation between graphite, diamond, and carbon dioxide: a new approach. *Geochim. Cosmochim. Acta*, 59(12), 2561-2572.

Riches A.J.V., Liu Y., Day J.M.D., Spetsius Z.V., and Taylor L.A., 2010, Subducted Oceanic Crust As Diamond Hosts Revealed By Garnets Of Mantle Xenoliths From Nyurbinskaya, Siberia, *Lithos*, 120(3-4), 368-378.

Rumble D., Miller M. F., Franchi I. A., and Greenwood R. C., 2007. Oxygen three-isotope fractionation lines in terrestrial silicate minerals: An inter-laboratory comparison of hydrothermal quartz and eclogitic garnet. Geochim. Cosmochim. Acta, 71(14), 3592-3600.

Russell A.K., Kitajima K., Strickland A., Medaris Jr. L.G., Schulze D.J., and Valley J.W., 2013. Eclogite-facies fluid infiltration: constraints from $\delta^{18}O$ zoning in granet. *Contrib. Mineral. Petrol.*, 165, 103-116.

Schmidberger S. S., Simonetti A., Heaman L. M., Creaser R. A., and Whiteford S., 2007. Lu–Hf, *in situ* Sr and Pb isotope and trace element systematics for mantle eclogites from the Diavik diamond mine: Evidence for Paleoproterozoic subduction beneath the Slave craton, Canada. *Earth Planet. Sci. Lett.*, *254*(1), 55-68.

Schmitz M. D., Bowring S. A., de Wit M. J., and Gartz V., 2004. Subduction and terrane collision stabilize the western Kaapvaal craton tectosphere 2.9 billion years ago. *Earth Planet. Sci Lett.*, 222(2), 363-376.

Schulze D.J., Valley J.W., and Spicuzza M.J., 2000. Coesite eclogites from the Roberts Victor kimberlite, South Africa. *Lithos*, 54, 23-32.

Schulze, D. J., Harte, B., Page, F. Z., Valley, J. W., Channer, D. M. D., and Jaques, A. L., 2013. Anticorrelation between low δ13C of eclogitic diamonds and high δ18O of their coesite and garnet inclusions requires a subduction origin. *Geology*, 41(4), 455-458.

Smart K.A., Heaman L.M., Chacko T., Simonetti A., Kopylova M., Mah D., and Daniels D., 2009. The origin of high-MgO diamond eclogites from the Jericho Kimberlite, Canada. *Earth Planet. Sci. Lett.*, 284, 527-537.

Smit K. V., Stachel T., Creaser R. A., Ickert R. B., DuFrane S. A., Stern R. A., and Seller M., 2014. Origin of eclogite and pyroxenite xenoliths from the Victor kimberlite, Canada, and implications for Superior craton formation. *Geochim. Cosmochim. Acta*, 125, 308-337.

Snyder G.A., Taylor L.A., Jerde E.A., Clayton R.N., Mayeda T.K., Deines P., Rossman G.R., and Sobolev N.V., 1995. Archean mantle heterogeneity and the origin of diamondiferous eclogites, Siberia: Evidence from stable isotopes and hydroxyl in garnet. *Amer. Min.*, 80, 799-809.

Snyder G.A., Taylor L.A., Crozaz G., Halliday A.N., Beard B.L., Sobolev V.N., and Sobolev N.V., 1997. The origins of Yakutian eclogite xenoliths. *J. Petrol.*, 38 (1), 85–113.

Snyder G. A., Taylor L. A., Beard B. L., Crozaz G., Halliday A. N., Sobolev V. N., and Sobolev N. V., 1998. Reply to a comment by D. Jacob et al. on 'The Origins of Yakutian Eclogite Xenoliths'. *J. Petrol.*, *39*(8), 1535-1543.

Shirey S.B., Carlson R.W., Richardson S.H., Menzies A., Gurney J.J., Pearson D.G., Harris J.W., and Wiechert U., 2001. Archean emplacement of eclogitic components into lithospheric mantle during formation of the Kaapvaal Craton. *Geophys. Res. Lett.*, 28(13), 2509-2512.

Shu Q., and Brey G. P., 2015. Ancient mantle metasomatism recorded in subcalcic garnet xenocrysts: Temporal links between mantle metasomatism, diamond growth and crustal tectonomagmatism. *Earth Planet. Sci. Lett.*, 418, 27-39.

Shu Q., Brey G. P., Gerdes A., and Hoefer H. E., 2014. Mantle eclogites and garnet pyroxenites–the meaning of two-point isochrons, Sm–Nd and Lu–Hf closure temperatures and the cooling of the subcratonic mantle. *Earth Planet. Sci. Lett.*, 389, 143-154.

Shu Q., Brey G. P., Gerdes A., and Hoefer H. E., 2013. Geochronological and geochemical constraints on the formation and evolution of the mantle underneath the Kaapvaal craton: Lu–Hf and Sm–Nd systematics of subcalcic garnets from highly depleted peridotites. *Geochim Cosmochim Acta*, 113, 1-20.

Sobolev V. N., Taylor L. A., Snyder G. A. and Sobolev N. V., 1994. International Geological Congress, Beijing: University of Beijing, Diamondiferous eclogites from the Udachnaya kimberlite pipe, p. 359. Yakutia. *Int. Geol. Rev.*, 36, 42–64

Sobolev N.V., Snyder G.A., Taylor L.A., Keller R.A., Yefimova E.S., Sobolev V.N., and Shimizu N., 1998. Extreme chemical diversity in the mantle during eclogitic diamond formation: evidence from 35 garnet and 5 pyroxene inclusions in a single diamond. *Int. Geol. Rev.*, 40(7), 567-578.

Spetsius Z.V., and Taylor L.A., 2008. Diamonds of Siberia: photographic evidence for their origin. Knoxville, TN: Tranquility Base Press, pp 278.

Spetsius Z.V., Taylor L.A., Valley J.W., Deangelis M.T., Spicuzza M., Ivanov A.D., and Banzerak V.I., 2008. Diamondiferous xenoliths from crustal subduction: garnet oxygen isotopes from the Nyurbinskaya pipe, Yakutia. *Euro. J. Mineral.*, 20, 375–385.

Stachel T., and Harris J.W., 2008. The origin of cratonic diamonds—constraints from mineral inclusions. *Ore Geol. Rev.*, 34(1), 5-32.

Stachel T., Aulbach S., Brey G.P., Harris J.W., Leost I., Tappert R., and Viljoen K.S. 2004. The trace element composition of silicate inclusions in diamonds: a review. *Lithos*, 77(1), 1-19.

Tappe S., Smart K. A., Pearson D. G., Steenfelt A., and Simonetti A., 2011. Craton formation in Late Archean subduction zones revealed by first Greenland eclogites. *Geology*, *39*(12), 1103-1106.

Tappert R., Stachel T., Harris J. W., Muehlenbachs K., Ludwig T., and Brey G. P., 2005. Subducting oceanic crust: the source of deep diamonds. *Geology*, 33(7), 565-568.

Taylor H. P., 1977, Water/rock interactions and the origin of H_2O in granitic batholiths. *J. Geol. Soc.*, 133(6), 509-558.

Taylor L.A., and Neal C.R., 1989. Eclogites with oceanic crustal and mantle signatures from the Bellsbank kimberlite, South Africa, Part I: Mineralogy, petrography, and whole-rock chemistry. *J. Geol.*, 97(5), 551-567.

Taylor L.A., Snyder G.A., Crozaz G., Sobolev V.N., Yefimova E.S., and Sobolev N.V., 1996. Eclogitic inclusions in diamonds: evidence of complex mantle processes over time. *Earth Planet. Sci. Lett.*, 142(3), 535-551.

Taylor L. A., Milledge H. J., Bulanova G. P., Snyder G. A., and Keller R. A., 1998. Metasomatic eclogitic diamond growth: evidence from multiple diamond inclusions. *Int. Geol. Rev.*, 40(8), 663-676.

Taylor L.A., Keller R.A., Snyder G.A., Wang W., Carlson W.D., Hauri E.H., McCandless T., Kim K-R., Sobolev N.V., and Bezborodov S.M., 2000. Diamonds and their mineral inclusions, and what they tell us: A detailed "pull-apart" of a diamondiferous eclogite. *Int. Geol. Rev.* 42(11), 959-983.

Tomlinson E.L., Jones A.P., and Harris J.W., 2006. Co-existing fluid and silicate inclusions in mantle diamond. *Earth Planet. Sci. Lett.*, 250(3), 581-595.

Turner G., Burgess R., and Bannon M., 1990. Volatile-rich mantle fluids inferred from inclusions in diamond and mantle xenoliths. *Nature*, 344(6267), 653-655.

Viljoen K.S., Schulze D.J., and Quadling A.G., 2005. Contrasting Group I and Group II eclogite xenolith petrogenesis: Petrological, trace-element and isotopic evidence from eclogite, garnet-websterite and alkremite xenoliths in the Kaalvallei Kimberlite, South Africa. *J. Petrol.*, 46(10), 2059-2090.

Wang S. J., Teng F. Z., Williams H. M., and Li S. G., 2012. Magnesium isotopic variations in cratonic eclogites: origins and implications. *Earth Planet. Sci. Lett.*, 359, 219-226.

Williams H. M., Nielsen S. G., Renac C., Griffin W. L., O'Reilly S. Y., McCammon C. A., Pearson N., Viljoen F., Alt J.C., and Halliday, A. N., 2009. Fractionation of oxygen and iron isotopes by partial melting processes: implications for the interpretation of stable isotope signatures in mafic rocks. *Earth Planet. Sci. Lett.*, 283(1), 156-166.

Zack T., Foley S.F., and Rivers T., 2002. Equilibrium and disequilibrium trace element partitioning in hydrous eclogites (Trescolmen, Central Alps). *J. Petrol.*, 43(10), 1947-1974.

Zhang H.F., Mattey D.P., Grassineau N., Lowry D., Brownless M, Gurney J. J., and Menzies M.A., 2000. Recent fluid processes in the Kaapvaal Craton, South Africa: coupled oxygen isotope and trace element disequilibrium in polymict peridotites. *Earth Planet. Sci. Lett.*, 176, 57-72.

Zheng Y.-F., 1993. Calculation of oxygen isotope fractionation in anhydrous silicate minerals. *Geochim. Cosmochim. Acta*, 57(5), 1079-1091.

Zheng Y. F., Fu B., Gong B., and Li L., 2003. Stable isotope geochemistry of ultrahigh pressure metamorphic rocks from the Dabie–Sulu orogen in China: implications for geodynamics and fluid regime. *Earth Sci. Rev.*, 62(1), 105-161.

FIGURES AND CAPTIONS

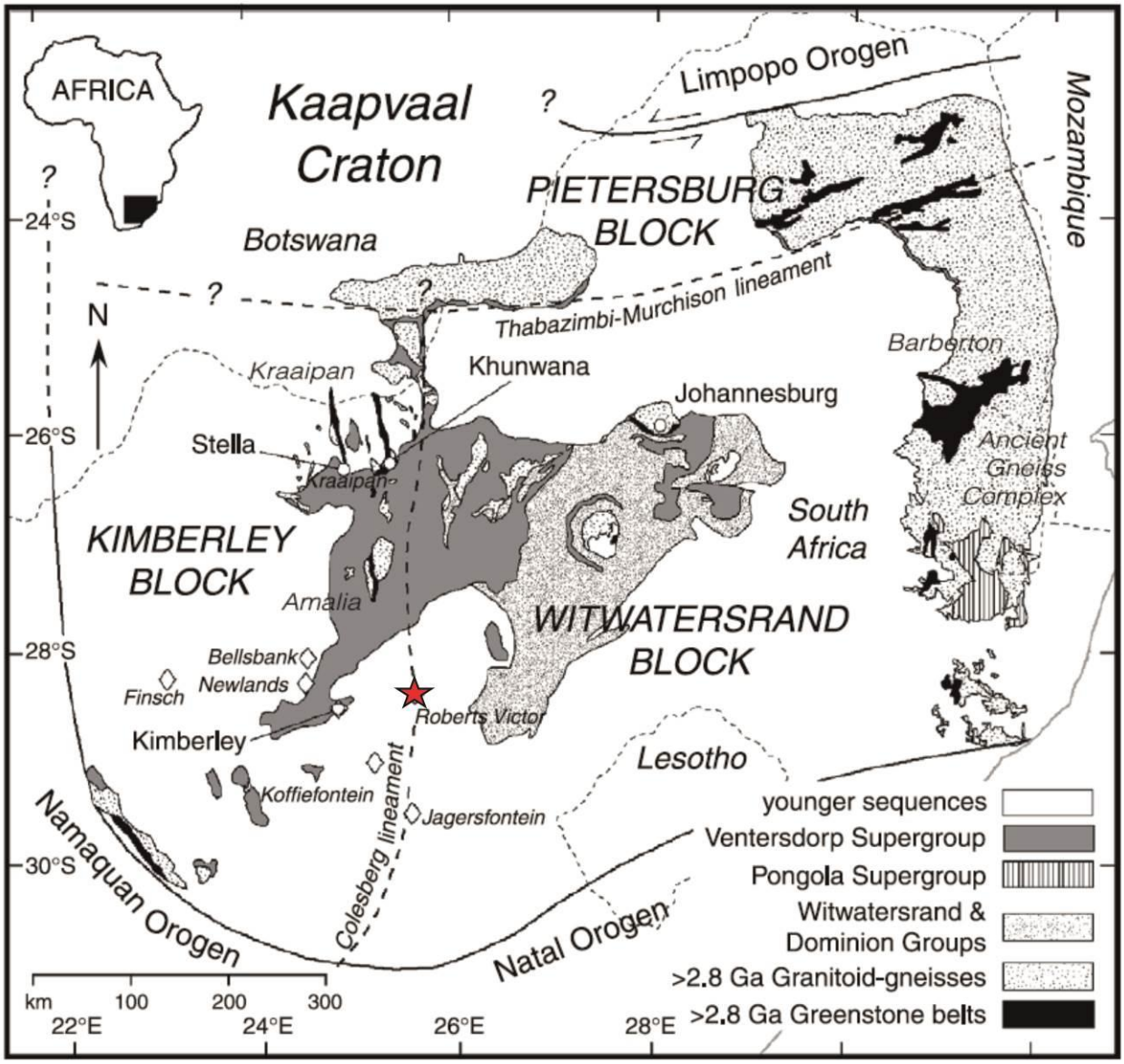

Figure 1: Simplified geological map of south eastern Africa. Location of the Roberts Victor mine is marked by the red star. This map depicts some of the major structural features within the Kaapvaal Craton. Image after Schmitz *et al.* (2004).

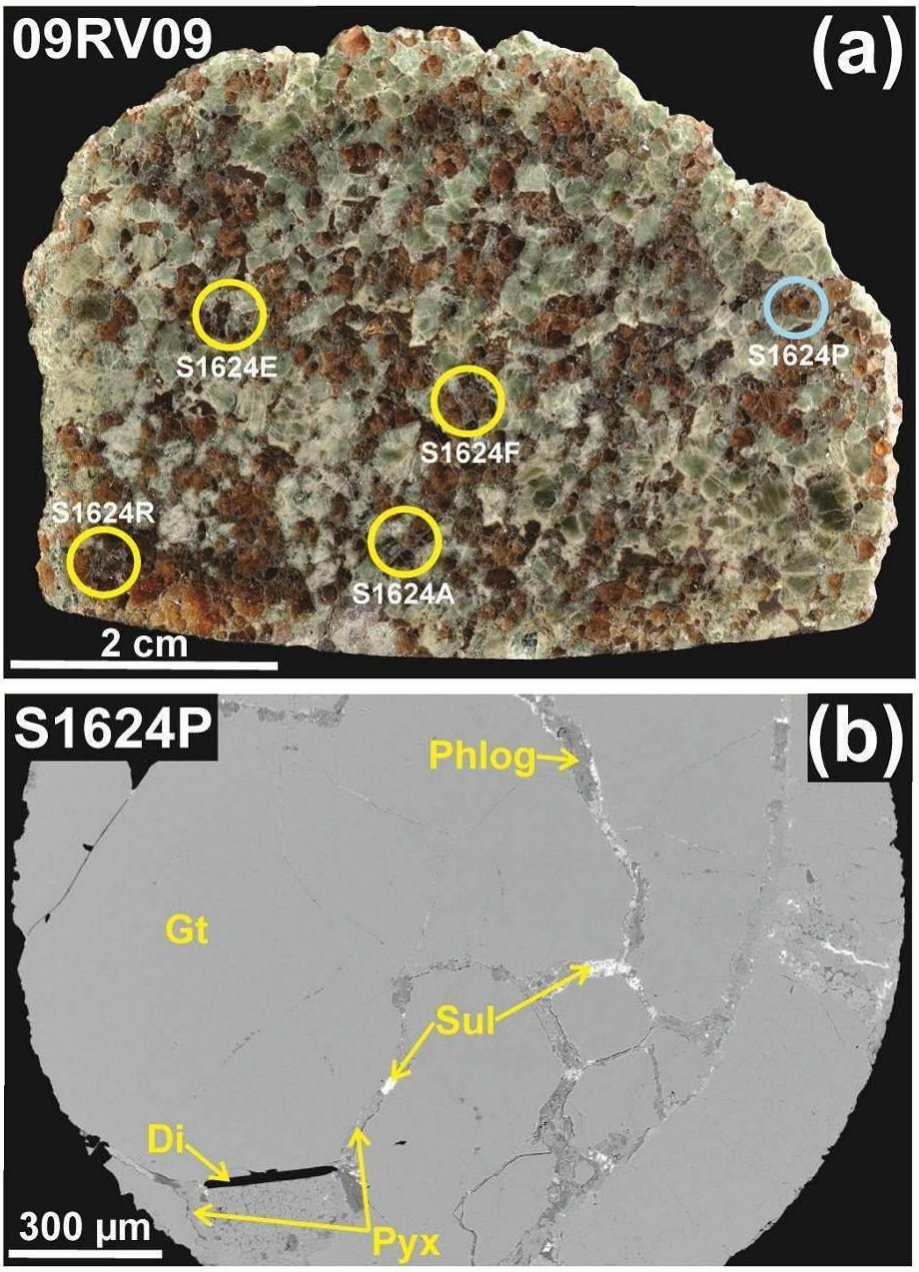

Figure 2: Hand-specimen (a) and back-scattered electron (BSE) image of 09RV09 (CCIM sample #S1624). Garnet and clinopyroxene modal abundances are heterogeneously distributed at the slice and hand-specimen scale. Sample portions extracted for *in* situ analyses are delineated by yellow and blue open-circles in (a), and S1624X labels correspond to sub-portion identifiers. The blue circle corresponds to a sample portion in which diamonds was preserved after polishing. Small diamond successfully retained *in situ* in sub-portion S1624P is intimately associated with garnet (b). Phase abbreviations are: Gt = garnet, Pyx = pyroxene, Phlog = phlogopite, Sul = sulphide, Di = diamond.

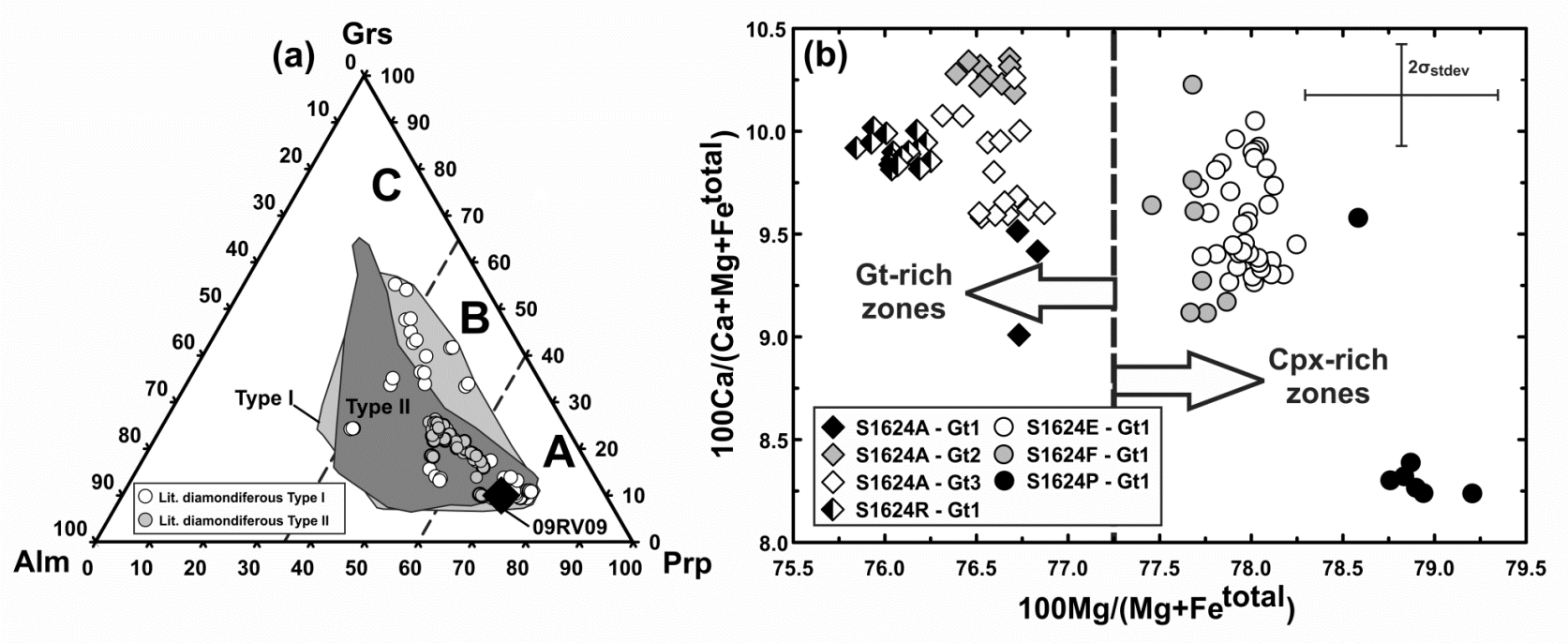

Figure 3: Garnet end-member (a; mol. %) and cation ratios (b). The range of intra- and inter-grain garnet compositions in 09RV09 shown in (a) is enclosed by a black diamond, and these data are compared with the range of garnet compositions reported in previous studies of Roberts Victor eclogites. Data fields in (a) delineate textural Group I and Group II eclogite xenoliths of Roberts Victor studied by Hatton (1978). Lit = literature, and corresponds to data reported by MacGregor and Manton (1986), O'Reilly and Griffin (1995), and Gréau *et al.* (2011). The range of intra- and inter-grain major-element cation values in garnets of 09RV09 is shown in (b), and the standard deviation (SD) was calculated via propagation of typical uncertainties on Ca, Mg, and Fe^{total} (this represents a minimum value as propagated uncertainties on other cations are not included).

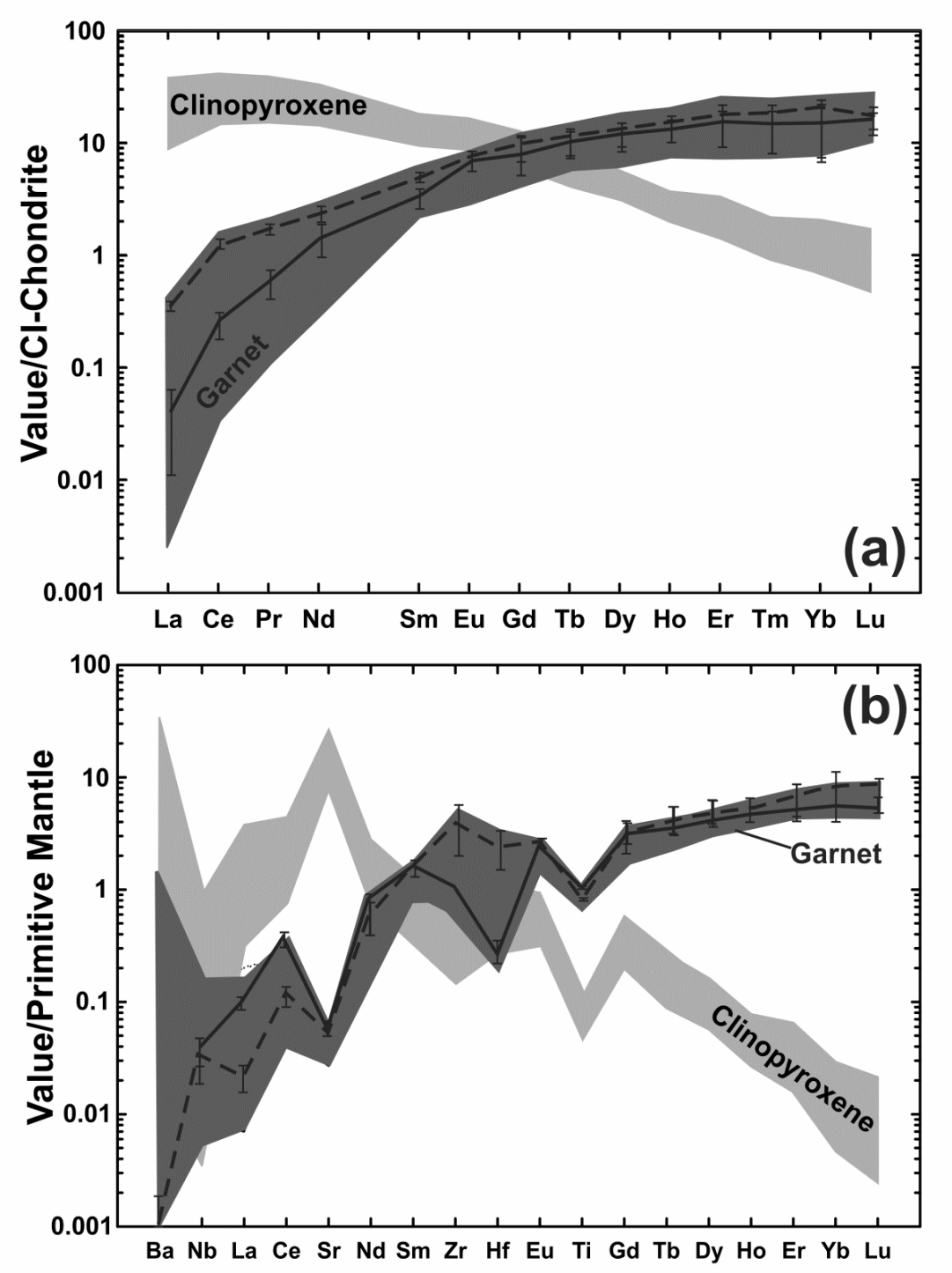

Figure 4: Rare-earth-element and extended trace-element abundances of 09RV09 minerals normalised to the values of CI-Chondrite and primitive mantle reported by McDonough and Sun (1995). Propagated uncertainties include 2σ precision values determined for each analytical point. Pm is not measured and is shown as an interpolated space between Nd and Sm (a).

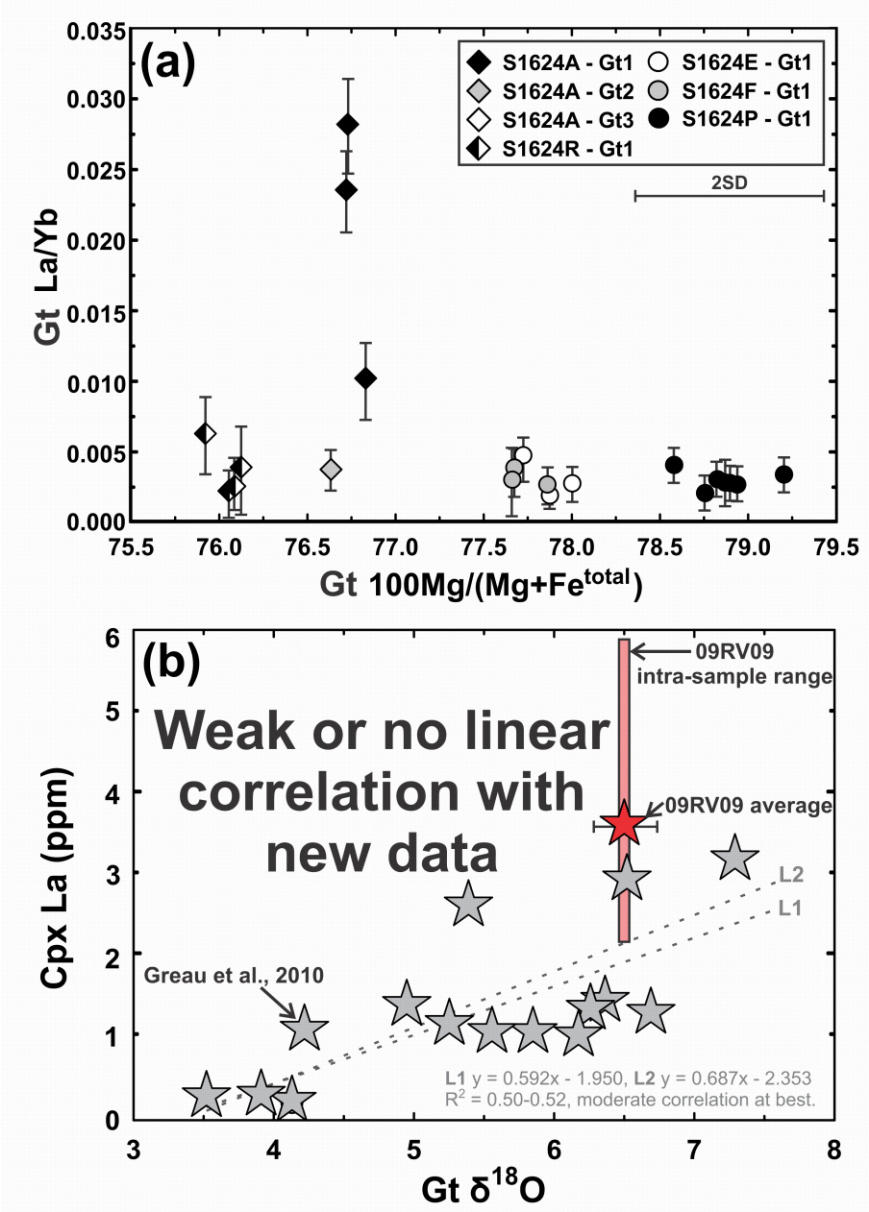

Figure 5: a) Garnet cation compositions and corresponding La/Yb. Propagated uncertainties on La/Yb reflect the 2σ internal precision determined for each analytical point. The typical uncertainty on 100Mg/(Mg+Fe^{total}) represents a minimum value as propagated uncertainties on other cation proportions (e.g., Si) are not included (where SD = standard deviation). b) Comparison of Roberts Victor garnet oxygen isotope compositions with La abundances of coexisting clinopyroxenes. Uncertainties on La abundances represent 2σ precision. Linear regressions of the data of Gréau *et al.* (2010) alone (L1), and incorporating the 09RV09 average (L2), are not strongly correlated (R^2 <<0.7). The 09RV09 clinopyroxene La abundance data range is depicted by the red bar; inclusion of all 09RV09 clinopyroxene La abundance data (rather than using a single average value) further reduces the correlation coefficient (R^2 <0.1).

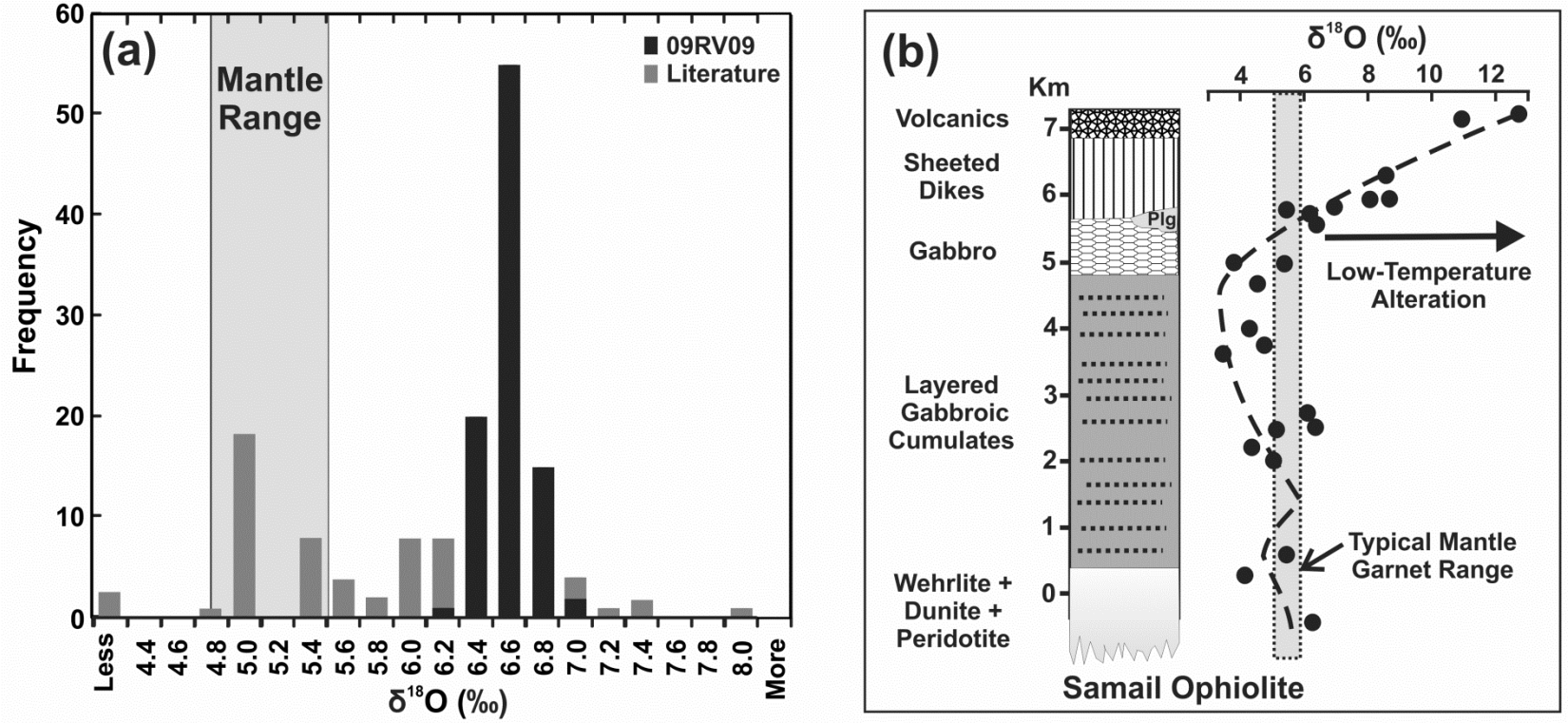

Figure 6: Histogram of oxygen isotope compositions determined for garnets of 09RV09 using ion probe techniques. Literature data reported for garnet separates of 62 Roberts Victor eclogite xenoliths were sourced from (Garlick *et al.*, 1971; MacGregor and Manton; 1986; Ongley *et al.*, 1987; Caporuscio, 1990; Schulze *et al.*, 2000; Gréau *et al.*, 2011) and the garnet mantle range is after Mattey *et al.*, (1994). A schematic illustration of the range of $\delta^{18}O$-compositions determined for samples of the Samail Ophiolite (b); where $\delta^{18}O$-compositions >+5.9 ‰ are associated with upper sections of oceanic crust altered at low-temperatures (<350 ºC; after Gregory and Taylor, 1981).

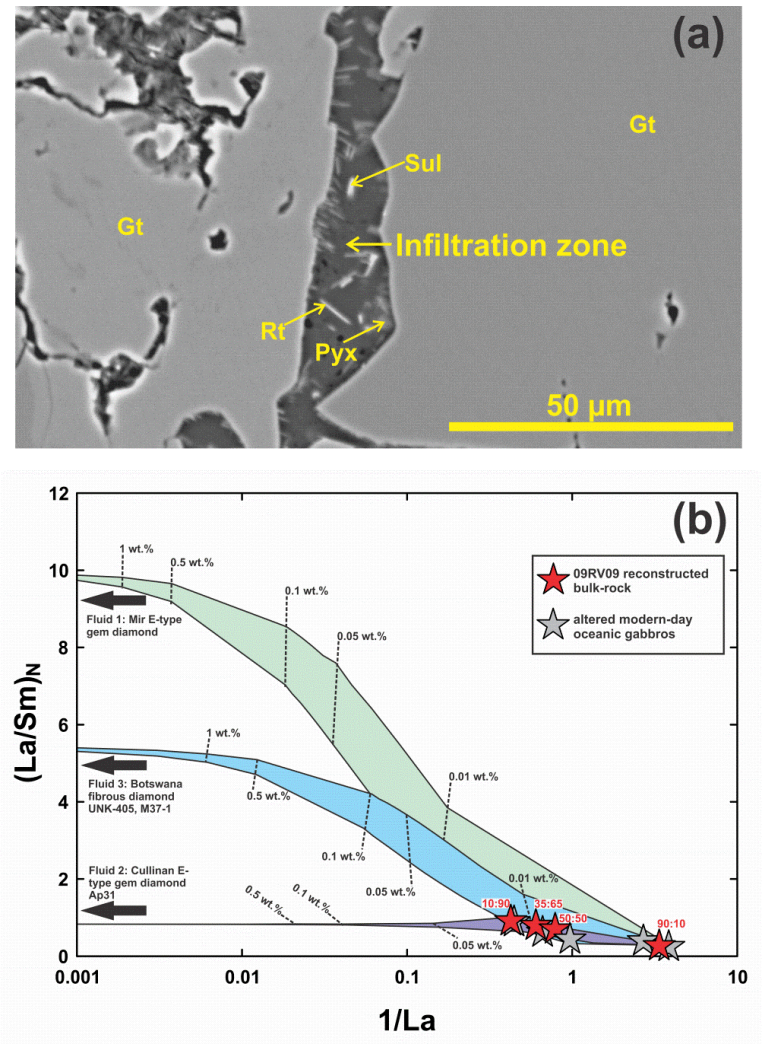

Figure 7: Infiltration and metasomatic modification of 09RV09. a) Narrow infiltration zone and associated metasomatic phases adjacent to garnet in 09RV09. Gt = garnet, Pyx = pyroxene, Rt = rutile, Sul = sulphide. The dark grey of the infiltration zone represent quenched material. b) Reciprocal La abundance (ppm) and CI-chondrite normalised La/Sm values of calculated bulk-rock reconstructions of 09RV09 over a range of garnet:clinopyroxene ratios compared with representative compositions reported for relatively fresh and altered gabbros of the slow-spreading SW Indian Ridge (Hart *et al.*, 1999; Bach *et al.*, 2001). Mixing products determined for the addition of fluids associated with diamond to these gabbroic compositions, which may approximate an eclogite protolith, are shown as shaded fields and the percentage of fluid is marked by dashed lines (refer to **supplementary materials** for further details). For visual clarity, the results of mixing calculations determined for F4 (a fluid with relatively low total REE abundances) are omitted from this image. Gt = garnet, Pyx = pyroxene, Sul = sulphide, Rt = rutile.

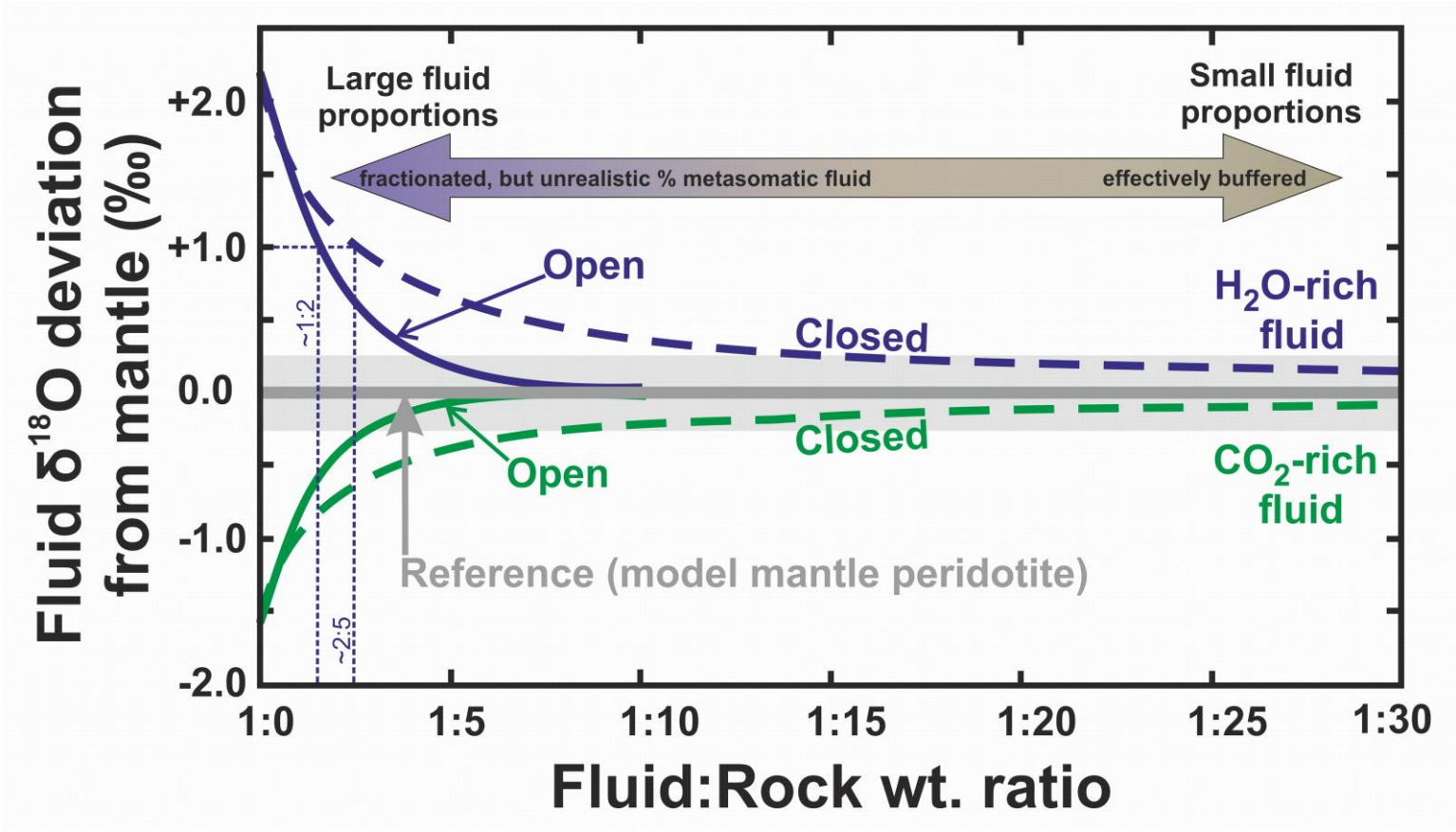

Figure 8: Model of the effect of closed- and open-system interaction between CO_2-rich and H_2O-rich metasomatic fluids and peridotite on the fluid $\delta^{18}O$-composition. Details of the model are given in the text. The ordinate of the figure is the difference between the fluid composition and a composition representing a completely rock-dominated system (e.g., where the fluid composition is fixed by the initial isotopic composition of the peridotite and the fractionation factor). The model curves asymptotically approach zero, where any initial ^{18}O-enrichment or depletion is effectively erased by equilibration with a large enough volume of rock. The grey region marks a ±0.25 ‰ band around the zero value, reflecting a composition that is effectively indistinguishable from one that is completely rock buffered. Under open-system conditions, and at fluid:rock ratios <1:10, the $\delta^{18}O$-value of the fluid is indistinguishable from the silicate mantle with which it is interacting.

884

885

886

887

888

889

890

891 -end-